CYK-4 regulates Rac, but not Rho, during cytokinesis

Yelena Zhuravlev[a], Sophia M. Hirsch[a], Shawn N. Jordan[b], Julien Dumont[c], Mimi Shirasu-Hiza[a], and Julie C. Canman[b,*]

[a]Department of Genetics and Development and [b]Department of Pathology and Cell Biology, Columbia University Medical Center, New York, NY 10032; [c]Institut Jacques Monod, CNRS, UMR 7592, Université Paris Diderot, Sorbonne Paris Cité, F-75205 Paris, France

ABSTRACT Cytokinesis is driven by constriction of an actomyosin contractile ring that is controlled by Rho-family small GTPases. Rho, activated by the guanine-nucleotide exchange factor ECT-2, is upstream of both myosin-II activation and diaphanous formin-mediated filamentous actin (f-actin) assembly, which drive ring constriction. The role for Rac and its regulators is more controversial, but, based on the finding that Rac inactivation can rescue cytokinesis failure when the GTPase-activating protein (GAP) CYK-4 is disrupted, Rac activity was proposed to be inhibitory to contractile ring constriction and thus specifically inactivated by CYK-4 at the division plane. An alternative model proposes that Rac inactivation generally rescues cytokinesis failure by reducing cortical tension, thus making it easier for the cell to divide when ring constriction is compromised. In this alternative model, CYK-4 was instead proposed to activate Rho by binding ECT-2. Using a combination of time-lapse in vivo single-cell analysis and *Caenorhabditis elegans* genetics, our evidence does not support this alternative model. First, we found that Rac disruption does not generally rescue cytokinesis failure: inhibition of Rac specifically rescues cytokinesis failure due to disruption of CYK-4 or ECT-2 but does not rescue cytokinesis failure due to disruption of two other contractile ring components, the Rho effectors diaphanous formin and myosin-II. Second, if CYK-4 regulates cytokinesis through Rho rather than Rac, then CYK-4 inhibition should decrease levels of downstream targets of Rho. Inconsistent with this, we found no change in the levels of f-actin or myosin-II at the division plane when CYK-4 GAP activity was reduced, suggesting that CYK-4 is not upstream of ECT-2/Rho activation. Instead, we found that the rescue of cytokinesis in CYK-4 mutants by Rac inactivation was Cdc42 dependent. Together our data suggest that CYK-4 GAP activity opposes Rac (and perhaps Cdc42) during cytokinesis.

INTRODUCTION

Rho-family small GTPases (Rho, Rac, and Cdc42) function as molecular switches: when GDP-bound, they are inactive, and when GTP-bound, they interact with cytoskeletal effectors to choreograph the cell shape changes required for complex cellular events such as cell motility, phagocytosis, and cytokinesis (Hall, 2012; Jordan and Canman, 2012; Mao and Finnemann, 2015; Ridley, 2015). Cytokinesis—the physical division of one cell into two—is driven by constriction of an actomyosin contractile ring, directed to form at the division plane after anaphase onset (AO) via Rho-family GTPase signaling. In most animal cells, assembly and constriction of the actomyosin contractile ring is downstream of Rho (O'Connell *et al.*, 1999; Bement *et al.*, 2005; Kamijo *et al.*, 2006), which is activated at the division plane by

the guanine-nucleotide exchange factor (GEF) epithelial cell transforming-2 (ECT-2), a human oncogene (Tatsumoto *et al.*, 1999; Kimura *et al.*, 2000; Kamijo *et al.*, 2006; D'Avino *et al.*, 2015). Once activated, Rho promotes both filamentous actin (f-actin) nucleation by a diaphanous-family formin (CYK-1 in *Caenorhabditis elegans*; hereafter, formin) and nonmuscle myosin-II (NMY-2 in *C. elegans*; hereafter, myosin-II) motor activation, which drive contractile ring assembly and power ring constriction (for review, see Pollard, 2010; Green *et al.*, 2012; D'Avino *et al.*, 2015). Rho activation during cytokinesis is opposed by the GTPase-activating protein (GAP) MP-GAP (RGA-3/4 in *C. elegans*), which promotes Rho's hydrolysis of GTP to GDP (Zanin *et al.*, 2013).

The role(s) for the Rho family GTPase Rac and the Rac GAP CYK-4 during cytokinesis are under debate. CYK-4 (HsCYK4/MgcRacGAP in humans, RacGAP50c in flies; hereafter, CYK-4) is essential for cytokinesis in nearly all cell types (Jantsch-Plunger *et al.*, 2000; Hirose *et al.*, 2001; Goldstein *et al.*, 2005), forms a complex called Centralspindlin with the kinesin MKLP-1/ZEN-4 (Mishima *et al.*, 2002; Pavicic-Kaltenbrunner *et al.*, 2007), and has been proposed to both inhibit Rac activation and promote Rho activation at the division plane via its GAP domain (Jantsch-Plunger *et al.*, 2000; D'Avino *et al.*, 2004; Canman *et al.*, 2008; Miller and Bement, 2009; Bastos *et al.*, 2012; Loria *et al.*, 2012; Cannet *et al.*, 2014; Zhang and Glotzer, 2015). In vitro, CYK-4 inactivates Rac and Cdc42 by promoting GTP hydrolysis but has little effect on the activity of Rho (Toure *et al.*, 1998; Jantsch-Plunger *et al.*, 2000; Bastos *et al.*, 2012). In vivo, CYK-4 has been proposed to inhibit Rac activity (D'Avino *et al.*, 2004; Yoshizaki *et al.*, 2004; Canman *et al.*, 2008; Bastos *et al.*, 2012; Cannet *et al.*, 2014), promote Rho-GTP turnover (or flux; Miller and Bement, 2009), and promote the activation of Rho by stimulating the GEF activity of ECT-2 during cytokinesis (Zhao and Fang, 2005; Loria *et al.*, 2012; Tse *et al.*, 2012; Zhang and Glotzer, 2015). Thus there is no consensus view on the mechanisms by which CYK-4 and/or Rac activity regulate cytokinesis.

To support the model in which CYK-4 negatively regulates Rac during cytokinesis in worms, flies, and cultured human cells, mutational disruption of the CYK-4 GAP domain leads to cytokinesis failure that can be rescued by reducing Rac activity (D'Avino *et al.*, 2004; Canman *et al.*, 2008; Bastos *et al.*, 2012; Cannet *et al.*, 2014). Cytokinesis failure in CYK-4 GAP-domain mutants can also be rescued by depletion of the Arp2/3 complex, a Rac effector, and branched f-actin nucleator in worms and cultured mammalian cells (Canman *et al.*, 2008; Cannet *et al.*, 2014). Moreover, in cultured mammalian cells, cytokinesis failure caused by CYK-4 GAP disruption can be rescued by depleting Rac effectors that promote cell substrate attachment such as PAK1 and ARHGEF7 (Bastos *et al.*, 2012) and the upstream Rac GEF Trio (Cannet *et al.*, 2014). Thus CYK-4 GAP-mediated inactivation of Rac at the division plane has been proposed to function in parallel to Rho activation to allow contractile ring constriction and promote efficient cytokinesis.

In contrast, CYK-4 has also been proposed to function during cytokinesis through the promotion of Rho activation by facilitating GTP turnover (flux) or by activating the Rho GEF ECT-2 (Zhao and Fang, 2005; Miller and Bement, 2009; Loria *et al.*, 2012; Tse *et al.*, 2012; Zhang and Glotzer, 2015). Although, in vitro, CYK-4 is not effective at promoting the GTP turnover of Rho (Toure *et al.*, 1998; Jantsch-Plunger *et al.*, 2000; Bastos *et al.*, 2012), in vivo mutations in the GAP domain have a strong effect on the width and stability of the zone of active GTP-bound Rho at the division plane in *Xenopus* embryos (Miller and Bement, 2009). This could be due to a direct effect on Rho activation or an indirect effect by modulating other Rho family members that compete for effectors and upstream regu-

lators, such as GAPs, GEFs, and guanosine nucleotide dissociation inhibitor (GDIs; e.g., Tatsumoto *et al.*, 1999; Machacek *et al.*, 2009; Boulter *et al.*, 2010; Garcia-Mata *et al.*, 2011). CYK-4 has also been proposed to promote Rho activation by stimulating the Rho GEF ECT-2 (Zhao and Fang, 2005; Zhang and Glotzer, 2015). This hypothesis was based on the findings that CYK-4/MgcRacGAP can bind ECT-2 (Somers and Saint, 2003; Yuce *et al.*, 2005; Burkard *et al.*, 2009; Wolfe *et al.*, 2009; Zhang and Glotzer, 2015) and that mutational disruption of the CYK-4 GAP domain can be suppressed by hyperactivating mutations in the ECT-2 GEF domain (Zhang and Glotzer, 2015). The same group also reported that CYK-4 disruption prevents the enrichment of f-actin and myosin-II at the division plane, which would be expected if CYK-4 activates ECT-2 and thus Rho activity during cytokinesis (Loria *et al.*, 2012). However, other studies could not confirm that CYK-4 GAP disruption leads to decreased levels of myosin-II at the division plane (Canman *et al.*, 2008; Zhang and Glotzer, 2015). Moreover, in vitro analysis found no change in ECT-2 GEF activity toward Rho in the presence or absence of CYK-4 (Zhang and Glotzer, 2015), although this negative result cannot rule out that additional factors may be needed. Thus, whereas CYK-4 has been proposed to play an essential role in ECT-2 and Rho activation, much of the evidence for this model is indirect.

Furthermore, in models that support a role for CYK-4 in Rho activation via ECT-2 (Loria *et al.*, 2012; Zhang and Glotzer, 2015), the finding that cytokinesis failure resulting from CYK-4 GAP disruption can be rescued by Rac inactivation is attributed to a general or "bypass" role for Rac (Loria *et al.*, 2012) in regulating cortical tension and opposing contractile ring constriction, as was found in *Dictyostelium* (Zhang and Robinson, 2005). Support for this model relies on the finding that reducing Rac activity could also rescue cytokinesis failure in a hypomorphic *ect-2(temperature-sensitive* [*ts*]) mutant background (Loria *et al.*, 2012). Yet, in vitro ECT-2 GEF activity can activate both Rho and Rac (Tatsumoto *et al.*, 1999); thus Rac depletion might rescue cytokinesis when ECT-2 activity is weakened by simply reducing competition with Rho for the GEF domain. Moreover, Rac disruption does not rescue cytokinesis failure when Aurora B kinase activity is compromised, which also regulates contractile ring constriction in a pathway parallel to CYK-4 during cytokinesis (Lewellyn *et al.*, 2011). Thus a general role for Rac in opposing contractile ring constriction in animal cells is not well supported.

The role for Cdc42 in animal cell cytokinesis is also controversial. Cdc42 is essential for polar body emission during meiotic cytokinesis in frog and murine embryos (Ma *et al.*, 2006; Zhang *et al.*, 2008; Wang *et al.*, 2013). However, disruption of Cdc42 does not block mitotic cytokinesis in most metazoan systems (Gotta *et al.*, 2001; Zhu *et al.*, 2011; Jordan *et al.*, 2016). Injection of constitutively active or dominant-negative forms of Cdc42 at very high levels (micromolar range) can disrupt mitotic cytokinesis in frog embryos (Drechsel *et al.*, 1997), and expression of constitutively active Cdc42 in dividing mammalian cultured cells leads to the assembly of a broader contractile ring but does not block cytokinesis (Zhu *et al.*, 2011). In asymmetrically dividing *C. elegans* embryos, Cdc42 regulates cell polarity and is required for robust contractile ring f-actin assembly, and its depletion leads to synthetic cytokinesis failure in embryos from a temperature-sensitive diaphanous-related formin mutant (Jordan *et al.*, 2016). Hence Cdc42 likely participates in animal cell cytokinesis but is not an essential player.

Here we examine the roles of Rac and the GAP CYK-4 in cytokinesis in the early *C. elegans* embryo. We find that, as shown previously, Rac inactivation rescues cytokinesis failure in a CYK-4 GAP mutant and to a lesser extent in a hypomorphic ECT-2 mutant. Rac disruption does not rescue the rate of contractile ring constriction
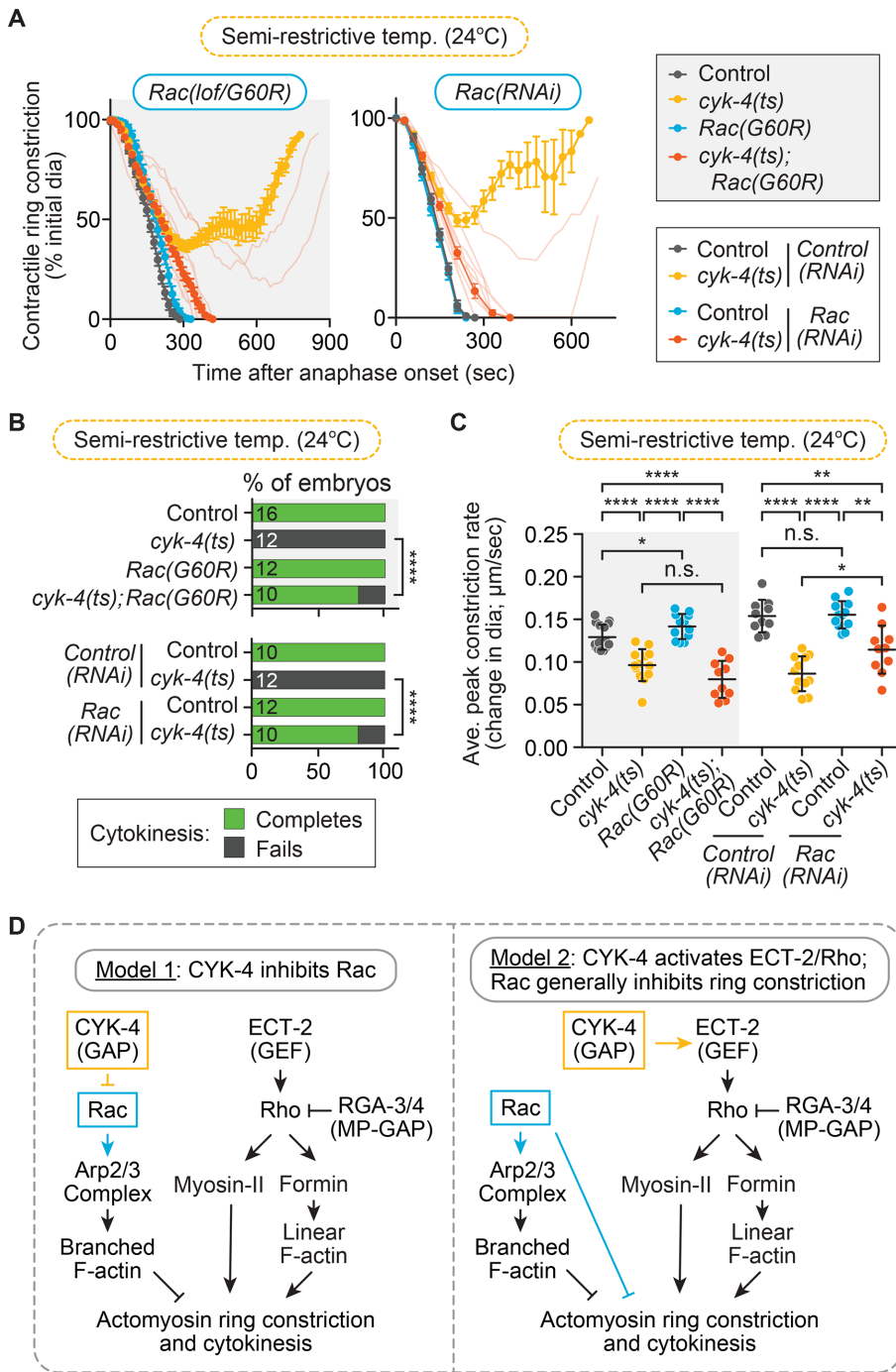
FIGURE 1: Rac disruption rescues cytokinesis failure in a CYK-4 GAP mutant. (A) Kinetic analysis of contractile ring constriction in control and *cyk-4(ts)* mutant 1-cell embryos at semirestrictive temperature (24°C) with and without *Rac(lof/G60R)* (left) and *Rac(RNAi)* (right). Mean ring diameter vs. time, with all replicates for the *cyk-4(ts); Rac(G60R or RNAi)* shown in the background in a more transparent shade of the same orange. Error bars represent SEM. (B) Cytokinesis failure and success rates for different genotypes in A. The number of embryos per genotype is indicated on each individual bar; *p* values were obtained by both Fisher's and Barnard's exact tests (Supplemental Table S3). (C) Average peak rate of contractile ring constriction plotted as change in diameter (μm/s; see *Materials and Methods* for image analysis). Error bars represent SD; *p* values were obtained by an unpaired, two-tailed Student's *t* test (Supplemental Table S3). (D) Current genetic models for the function of CYK-4 and Rac during cytokinesis. n.s., *p* ≥ 0.05; *p < 0.05; **p < 0.01; ****p < 0.0001.

in CYK-4 or ECT-2 mutants, and we find that Rac disruption–mediated rescue of cytokinesis failure in CYK-4 mutants depends on Cdc42. We do not find evidence that Rac activity generally opposes contractile ring constriction, as Rac inactivation did not rescue the rate of cytokinesis failure in embryos with mutations in the Rho effectors diaphanous formin or the motor myosin-II. Furthermore, disrupting CYK-4 activity did not lead to a reduction in the total levels of contractile ring f-actin or myosin-II at the division plane, indicating that CYK-4 is unlikely to act upstream of ECT-2–mediated activation of Rho. Instead, we propose that, at least in the early *C. elegans* embryo, ECT-2 activity may promote Rac activation and thus in part negatively regulate cytokinesis. Together our data support a model in which CYK-4 functions to inhibit Rac activity (and potentially Cdc42) and does not participate directly in Rho activation; our data also do not suggest a nonspecific or bypass role for Rac in opposing contractile ring constriction.

RESULTS

We first sought to confirm that cytokinesis failure due to mutational disruption of the CYK-4 GAP domain could be rescued by reducing Rac activity. To do this, we performed time-lapse image analysis of cytokinesis in the one-cell *C. elegans* embryo, with and without Rac disruption, in a temperature-sensitive CYK-4 GAP-domain mutant (E448K) background (Canman *et al.*, 2008), hereafter, *cytokinesis defect 4* (*cyk-4*) *(ts)*. Imaging was done at the semirestrictive temperature (24°C), where contractile ring ingression progresses further in *cyk-4(ts)* mutant embryos than at fully restrictive temperature but cytokinesis fails 100% of the time in the *cyk-4(ts)* mutant alone (Figure 1, A and B). Rac activity was disrupted in two ways: 1) with feeding RNA interference (RNAi) and 2) with a loss-of-function (lof) Rac/CED-10 GTPase mutant (G60R; *ced-10(n3246)*; hereafter, *Rac(G60R)*; Reddien and Horvitz, 2000; Sun *et al.*, 2012; Cabello *et al.*, 2014) that, based on an identical G60R mutation in the closely related KRas, renders the small GTPase stuck in the GTP-bound state but unable to interact with effectors, GAPs, or GEFs (Gremer *et al.*, 2011). As expected, 100% of control, *control(RNAi)*, *Rac(RNAi)*, and *Rac(G60R)* single-mutant embryos successfully completed cytokinesis (16 of 16, 10 of 10, 12 of 12, and 12 of 12 embryos divide, respectively), whereas 100% of *cyk-4(ts)* and *cyk-4(ts); control(RNAi)*

embryos failed in cytokinesis at this temperature (0 of 12 and 0 of 12 embryos divide, respectively; Figure 1, A and B). In contrast, cytokinesis was significantly rescued (Fisher's and Barnard's exact tests; *p* values in Supplemental Table S3) in *cyk-4(ts); Rac(RNAi)* and *cyk-4(ts); Rac(G60R)* double mutant embryos (8 of 10 embryos divide for both genotypes; Figure 1, A and B). To test whether this rescue is conserved in other cell divisions, we also investigated whether Rac disruption could rescue cytokinesis failure in the AB and P1 blastomeres of two-cell *cyk-4(ts)* embryos (Supplemental Figure S1C). We found that both AB and P1 blastomeres fail cytokinesis in *cyk-4(ts)* two-cell embryos at a lower rate than in one-cell embryos (4 of 19 AB cells and 12 of 20 of P1 cells divide at semirestrictive temperature, 25.5°C in this case) (Supplemental Figure S1C). Nonetheless, cytokinesis failure was significantly rescued (Fisher's and Barnard's exact tests; *p* values in Supplemental Table S3) in both blastomeres of *cyk-4(ts); Rac(G60R)* double-mutant two-cell embryos (12 of 14 AB cells and 16 of 16 P1 cells divide successfully; Supplemental Figure S1C). Thus Rac inhibition rescues cytokinesis failure due to mutational disruption of the CYK-4 GAP domain in both one- and two-cell *C. elegans* embryos. This result supports a model in which CYK-4 GAP activity inhibits Rac activation during cytokinesis but does not rule out the possibility that Rac is a general inhibitor of contractile ring constriction (Figure 1D).

We next sought to determine whether Rac disruption can also rescue the slowed rate of contractile ring constriction observed in one-cell *cyk-4(ts)* embryos. Rac disruption by RNAi or the G60R mutation either did not significantly change or only mildly increased the rate of contractile ring constriction in both control and *cyk-4(ts)* embryos (Figure 1C; unpaired Student's *t* test; *p* values in Supplemental Table S3). Thus Rac disruption rescues the extent of contractile ring constriction but overall does not significantly rescue the rate of ring constriction in *cyk-4(ts)* mutants (Supplemental Table S3; Loria *et al.*, 2012). This result suggests that CYK-4 (and/or Rac) could play an independent role in regulating the rate of ring constriction, potentially by further activating ECT-2 (and thus Rho) at the division plane, as proposed in this system (Figure 1D; Tse *et al.*, 2012; Zhang and Glotzer, 2015). This result could also support a model in which Rac disruption rescues cytokinesis in *cyk-4(ts)* mutant embryos via a nonspecific or "bypass" pathway (e.g., Loria *et al.*, 2012; Zhang and Glotzer, 2015).

The main argument proposed against Rac as a specific target of CYK-4 is twofold: first, that Rac is a general inhibitor of ring constriction, and its depletion might nonspecifically rescue cytokinesis failure; and second, that CYK-4's true target is ECT-2. In the first part of the argument, Rac disruption has been proposed to allow successful cytokinesis in *cyk-4(ts)* embryos via a "bypass" mechanism that generally reduces cortical tension and makes it easier to complete cytokinesis when the contractile ring is weakened (Loria *et al.*, 2012; Figure 1D). We set out to resolve whether Rac disruption can generally rescue cytokinesis failure when ring constriction is weakened, by combining *Rac(RNAi)* or *Rac(lof)* with other mutants in the ECT-2/Rho pathway that would also compromise the integrity of the contractile ring. If disrupting Rac generally facilitates contractile ring constriction, then *Rac(lof)* should rescue cytokinesis failure when downstream targets of ECT-2/Rho are disrupted to weaken the contractile ring. Thus we next tested whether Rac disruption could rescue cytokinesis failure in a fast-acting *ts* mutant that affects the *C. elegans* diaphanous-related formin actin-nucleator CYK-1 (hereafter, *formin(ts)*), which is required to nucleate f-actin in the contractile ring and is activated downstream of Rho (Jordan and Canman, 2012; Jordan *et al.*, 2016; Davies *et al.*, 2014; Figure 1D). For this experiment, *formin(ts)* 1-cell embryos were imaged at the semi-

restrictive temperature (23.5°C), at which *formin(ts)* mutants alone can undergo partial contractile ring constriction but fail in cytokinesis 100% of the time (0 of 11 embryos divide; Figure 2, A and C; Jordan *et al.*, 2016). Of importance, at this semirestrictive temperature, cytokinesis failure in *formin(ts)* embryos can be fully rescued by depletion of other negative regulators of contractile ring constriction (e.g., septin; Jordan *et al.*, 2016). We found that at this temperature, *formin(ts); Rac(G60R)* mutants still failed in cytokinesis 100% of the time (0 of 10 embryos divide) and underwent even less contractile ring constriction than in the *formin(ts)* mutant alone (Figure 2, A and C). This result suggests that disrupting Rac activity does not significantly rescue cytokinesis failure in *formin(ts)* mutant embryos (Fisher's and Barnard's exact tests; *p* values in Supplemental Table S3). We next examined whether Rac disruption could enhance the rate of cytokinesis failure in *formin(ts)* mutant embryos at the semipermissive temperature (18.5°C), at which all *formin(ts)* mutant embryos successfully complete cytokinesis (13 of 13 embryos divide; Figure 2, B and D; Jordan *et al.*, 2016). At semipermissive temperature, *formin(ts); Rac(G60R)* embryos exhibited mild cytokinesis failure (10 of 12 embryos divide; Figure 2, B and D), although this was not statistically significant (Fisher's and Barnard's exact tests; *p* values in Supplemental Table S3). The rate of contractile ring constriction was significantly slower in *formin(ts)* mutant embryos than in control embryos at both semirestrictive and semipermissive temperatures, but this rate was not affected by the *Rac(G60R)* mutation (Figure 2, E and F; unpaired Student's *t* test; Supplemental Table S3). Thus perturbing Rac activity does not rescue cytokinesis failure when the contractile ring is weakened by reduced formin/CYK-1 activity.

We next tested whether Rac disruption could rescue cytokinesis failure when the actin-based motor NMY-2 is weakened, which drives contractile ring constriction downstream of Rho (Figure 1D). For this experiment, we used a fast-acting *myosin-II(ts)* allele (Liu *et al.*, 2010; Davies *et al.*, 2014) and imaged at the semirestrictive temperature (25.5°C), at which *myosin-II(ts)* single-mutant one-cell embryos can undergo some contractile ring constriction but fail in cytokinesis 100% of the time (0 of 13 embryos divide; Figure 3, A and C; Jordan *et al.*, 2016). Using the *Rac(G60R)* mutation, we found that at this temperature, all *myosin-II(ts); Rac(G60R)* embryos fail in cytokinesis (0 of 10 embryos divide) and undergo reduced contractile ring constriction relative to the *myosin-II(ts)* mutants alone (Figure 3, A and C). This result suggests that disrupting Rac activity does not significantly change the rate of cytokinesis failure in *myosin-II(ts)* mutant embryos (Fisher's and Barnard's exact tests; *p* values in Supplemental Table S3). We next examined the effect of Rac disruption on *myosin-II(ts)* mutant embryos at the semipermissive temperature (22.5°C), where the *myosin-II(ts)* mutant embryos undergo contractile ring constriction more slowly but cytokinesis is always successful (13 of 13 embryos divide; Jordan *et al.*, 2016). At semipermissive temperature, most *myosin-II(ts); Rac(G60R)* embryos complete cytokinesis (9 of 10 embryos divide; Figure 3, B and D). We also found that the rate of contractile ring constriction was significantly slower in *myosin-II(ts)* mutant embryos than in control embryos at both semirestrictive and semipermissive temperatures, and this constriction rate was not affected by the *Rac(G60R)* mutation (Figure 3, E and F; unpaired Student's *t* test; Supplemental Table S3). Thus perturbing Rac activity does not significantly rescue cytokinesis failure or the rate of contractile ring constriction when myosin-II activity is weakened (Supplemental Table S3). Together with a lack of rescue upon Rac disruption when formin (Figure 2) or Aurora B (Lewellyn *et al.*, 2011) activity is weakened, these data suggest that Rac disruption is not a simple bypass mechanism that
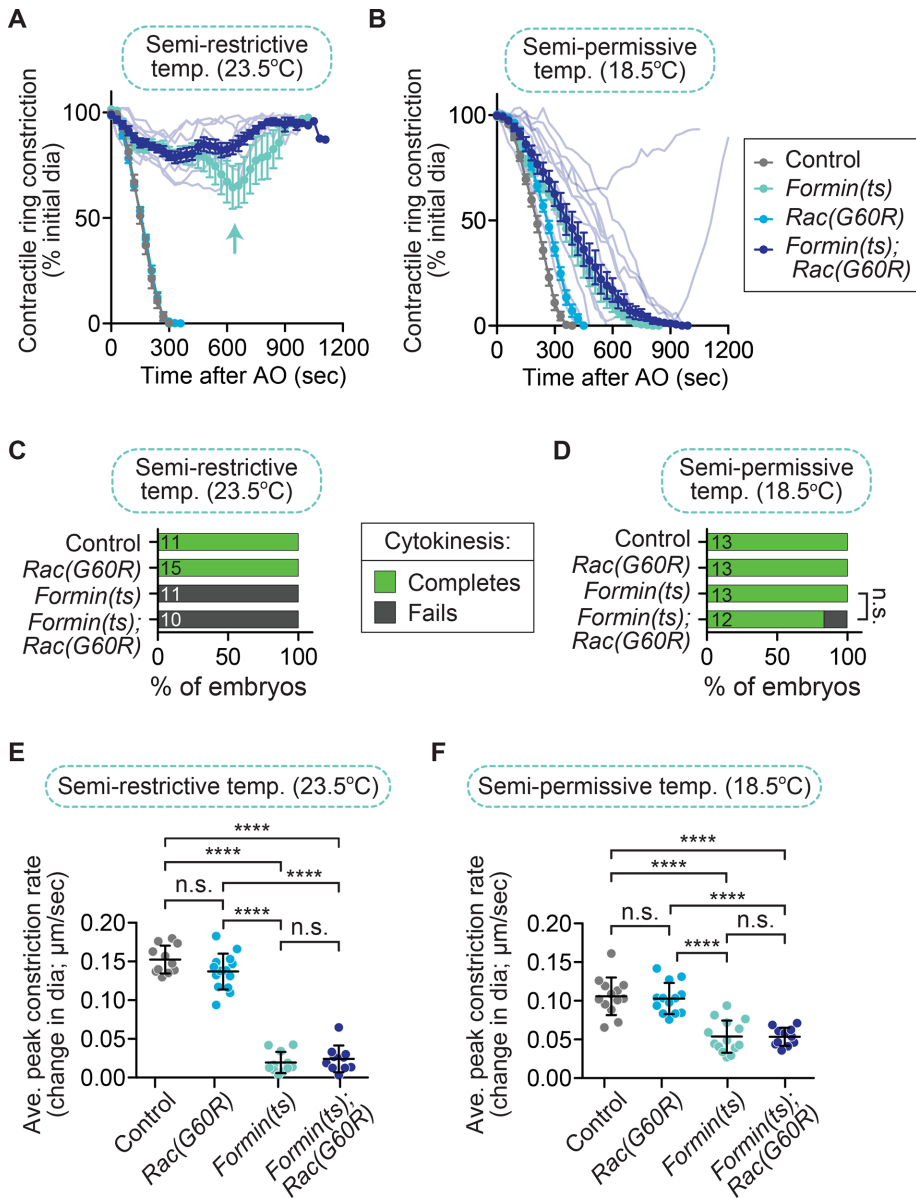
FIGURE 2: Rac disruption does not rescue cytokinesis failure in *formin(ts)* embryos. (A, B) Kinetic analysis of contractile ring constriction in control and *formin(ts)* mutant one-cell embryos with and without *Rac(G60R),* dividing at (A) semirestrictive (23.5°C) and (B) semipermissive (18.5°C) temperature. Mean ring diameter vs. time, with all replicates for the *formin(ts); Rac(G60R)* double mutant in a more transparent shade of the same dark blue. Error bars represent SEM. The aqua arrow in A shows the more persistent attempt at contractile ring constriction seen in *formin(ts)* single-mutant embryos but not in *formin(ts); Rac(G60R)* double-mutant embryos. (C, D) Cytokinesis failure and success rates for different genotypes at (C) semirestrictive and (D) semipermissive temperature. The number of embryos per genotype is indicated on each individual bar; *p* values were obtained by both Fisher's and Barnard's exact tests (Supplemental Table S3). (E, F) Average peak rate of contractile ring constriction plotted as the change in diameter (μm/s) when the rate of ingression peaks from ~90–50% ring constriction (or the point of maximum contractile ring constriction when embryos did not constrict to 50% of the initial cell diameter) at (E) semirestrictive and (F) semipermissive temperature. Error bars represent SD; *p* values were obtained by an unpaired, two-tailed Student's *t* test (Supplemental Table S3). n.s., $p \geq 0.05$; ****$p < 0.0001$.

facilitates completion of contractile ring constriction. Instead, our and others' genetic results suggest that Rac disruption specifically suppresses cytokinesis failure when CYK-4 (or ECT-2) is reduced (D'Avino et al., 2004; Canman et al., 2008; Bastos et al., 2012; Loria et al., 2012; Cannet et al., 2014).

To support the hypothesis that Rac disruption rescues cytokinesis failure via a non-specific mechanism, it was reported that Rac inhibition was also able to rescue cytokinesis failure of a slow-acting *ect-2* allele (*ax751ts*; hereafter, *ect-2(ts)*; Loria et al., 2012); we next sought to confirm this result. Loria et al. (2012) reported that *ect-2(ts)* mutant one-cell embryos fail in cytokinesis at a high frequency (~97%) after a prolonged (8+ h) up-shift to restrictive temperature and that this cytokinesis failure rate was reduced to ~35% in *ect-2(ts); Rac(V190G)* double-mutant embryos. This hypomorphic *ect-2(ts)* mutation is not a fast-acting ts allele and results from a single-residue substitution in the PH domain of ECT-2 (Zonies et al., 2010). More-over, embryos from this *ect(ts)* allele were first published to have a low frequency of cytokinesis failure after prolonged upshift to restrictive temperature, although the precise cytokinesis failure rate frequency was not re-ported (Zonies et al., 2010). We determined the rate of cytokinesis failure in this *ect-2(ts)* mutant background by monitoring the suc-cess or failure of cytokinesis in one-cell em-bryos after prolonged upshifts (12+ h) of *ect-2(ts)* mutants to the restrictive tempera-ture (26°C). In our hands, one-cell embryos from this *ect-2(ts)* mutant failed in cytokine-sis at a rate of only 38% (8 of 13 embryos divide; Figure 4, A and C). *ect-2(ts)* mutant embryos that failed in cytokinesis exhibited a significantly slower rate of contractile ring constriction than *ect-2(ts)* mutant embryos that successfully completed cytokinesis, but the overall rate of contractile ring constric-tion in *ect-2(ts)* mutants was unchanged by *Rac(RNAi)* (Figure 2B; unpaired Student's *t* test; Supplemental Table S3). Although the rate of cytokinesis failure in *ect-2(ts)* mutant embryos was low, in agreement with the re-sults of Zonies et al. (2010), we confirmed that cytokinesis failure could be partially suppressed by Rac disruption (Loria et al., 2012), as *ect-2(ts); Rac(RNAi)* embryos failed in cytokinesis at a rate of 17% (10 of 12 em-bryos divide; Figure 4, A and C). Based on either a Fisher's exact test or a Barnard's ex-act test, this rescue was not statistically sig-nificant (*p* values in Supplemental Table S3). We also investigated whether Rac disruption could rescue cytokinesis failure in the AB and P1 blastomeres of two-cell *ect-2(ts)* em-bryos with and without Rac depletion (Figure 4E). We found that 100% of both AB and P1 blastomeres successfully completed cytoki-nesis in *ect-2(ts); control(RNAi)* and *ect(ts); Rac(RNAi)* embryos, even after a 12-h upshift to restrictive temperature (12 of 12 of both AB and P1 cells divide in *ect-2(ts); Control(RNAi)* embryos; 14 of 14 AB cells and 16 of 16 P1 cells divide in *ect-2(ts); Rac(RNAi)* two-cell embryos, respectively; Figure 4E). The lack of cytokinesis failure in
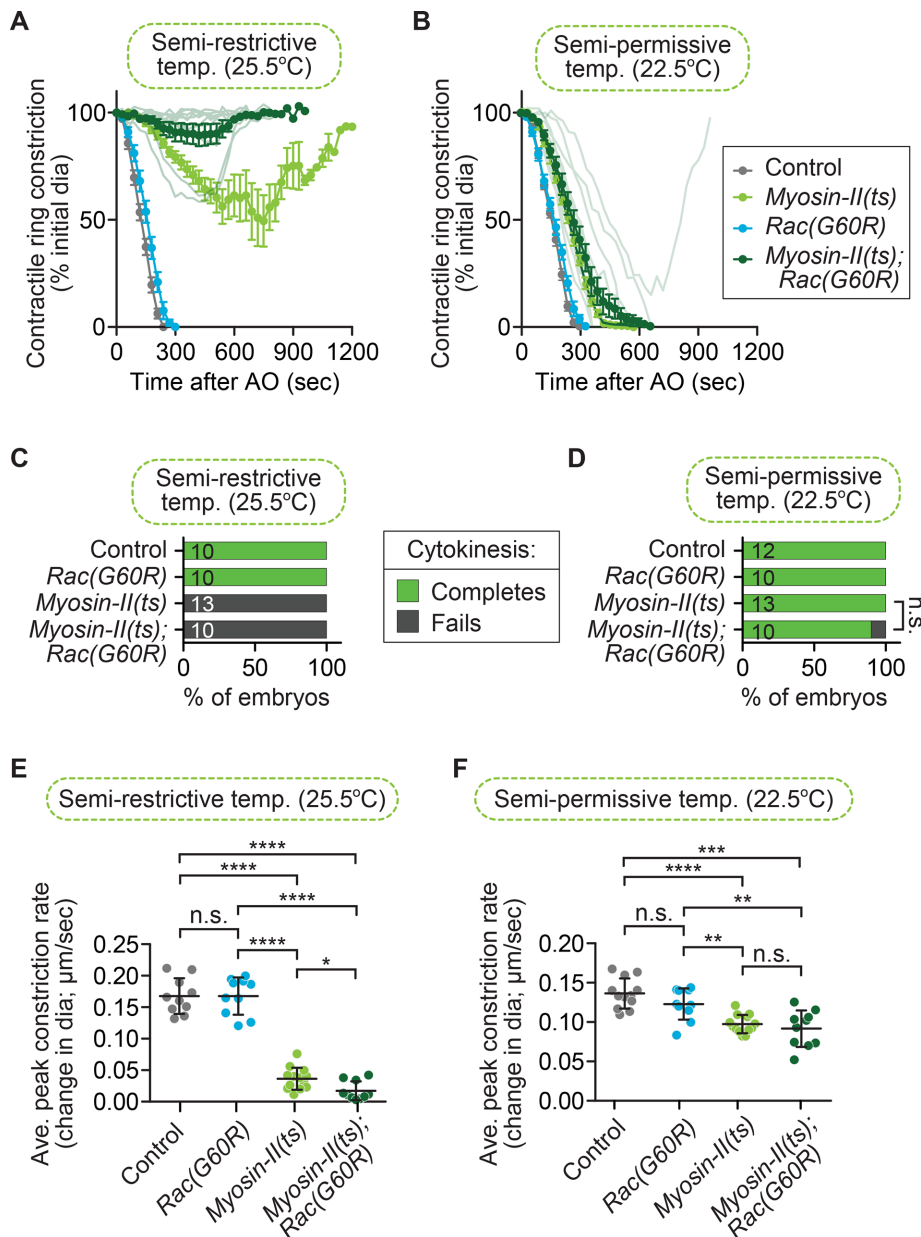
FIGURE 3: Rac disruption does not rescue cytokinesis failure in *myosin-II(ts)* embryos. (A, B) Kinetic analysis of contractile ring constriction in control and *myosin-II(ts)* mutant one-cell embryos with and without *Rac(G60R)*, dividing at (A) semirestrictive (25.5°C) and (B) semipermissive (22.5°C) temperature. Mean ring diameter vs. time, with all replicates for the *myosin-II(ts); Rac(G60R)* double mutant in a more transparent shade of forest green. Error bars represent SEM. (C, D) Cytokinesis failure and success rates for different genotypes at (C) semirestrictive and (D) semipermissive temperature. The number of embryos per genotype is indicated on each individual bar; *p* values were obtained by both Fisher's and Barnard's exact tests (Supplemental Table S3). (E, F) Average peak rate of contractile ring constriction, plotted as the change in diameter (μm/s) at (E) semirestrictive and (F) semipermissive temperature. Error bars represent SD; *p* values were obtained by an unpaired, two-tailed Student's *t* test (Supplemental Table S3). n.s., *p* ≥ 0.05; **p* < 0.05; ***p* < 0.01; ****p* < 0.001; *****p* < 0.0001.

Because we saw a lower rate of cytokinesis failure in the *ect-2(ts)* mutant and a lower rate of rescue after Rac disruption by RNAi than observed by Loria *et al.* (2012), we obtained the strains they used to test whether there could be strain variation between two labs. We found that their *ect-2(ts)* mutants still completed cytokinesis at a higher rate in our hands when upshifted to restrictive temperature for at least 12 h (52%, or 25 of 48 embryos divide here vs. ~3% in their work; Figure 4D), again more similar to the low cytokinesis failure rate of this mutant strain originally reported by Zonies *et al.* (2010). We also confirmed that the rate of cytokinesis failure was partially rescued in *ect-2(ts); Rac(V190G)* double mutants (14 of 19 embryos divide; Figure 4D). *Rac(V190G)* is a mild lof allele (*n1993*) that affects the CAAX box and thus likely affects Rac association with the plasma membrane (Kinsella *et al.*, 1991; Reddien and Horvitz, 2000; Shakir *et al.*, 2006; Roberts *et al.*, 2008; Steffen *et al.*, 2013). Although we do not observe the same high rate of cytokinesis failure in the *ect-2(ts)* mutant after prolonged upshifts to restrictive temperature as reported by Loria *et al.* (2012), possibly due to environmental effects, we observed a similar rescue of cytokinesis failure rates in *ect-2(ts); Rac(RNAi)* and *ect-2(ts); Rac(V190G)* embryos. Thus reducing Rac activity can partially rescue cytokinesis failure when ECT-2 activity is compromised, although to a lesser extent than in *cyk-4(ts)* mutants (e.g., Figure 1; Canman *et al.*, 2008; Loria *et al.*, 2012) and not to statistically significant levels (Supplemental Table S3).

The second part of the argument against Rac as a specific target of CYK-4 is that the main target of CYK-4 is ECT-2, which then activates Rho. This is largely based on the findings that 1) CYK-4 and ECT-2 from various species can interact in biochemical assays (Somers and Saint, 2003; Yuce *et al.*, 2005; Burkard *et al.*, 2009; Wolfe *et al.*, 2009; Kim *et al.*, 2014; Zou *et al.*, 2014; Zhang and Glotzer, 2015), and 2) a *C. elegans* gain-of-function ECT-2 mutation can rescue cytokinesis failure caused by a lof CYK-4 GAP mutation (Figure 1D; Zhang and Glotzer, 2015). If CYK-4 is upstream of ECT-2, then reducing CYK-4 activity should lead to a reduction in ECT-2–mediated Rho activation and Rho

two-cell *ect-2(ts)* embryos is likely due to the hypomorphic nature of this allele (Zonies *et al.*, 2010), although we cannot rule out the possibility that ECT-2 may play less of a role during cytokinesis in two-cell embryos than it does in one-cell embryos. Thus our data suggest that depletion of Rac by RNAi can partially rescue cytokinesis failure in one-cell embryos from *ect-2(ts)* mutants, although this rescue is not statistically significant (Supplemental Table S3).

effector accumulation at the division plane. To test this, we quantified the levels of downstream Rho targets green fluorescent protein (GFP::myosin-II [GFP::NMY-2; Munro *et al.*, 2004]) and a reporter for f-actin, GFP::utrophin[actin-binding domain] (GFP::UtrABD; Burkel *et al.*, 2007; Tse *et al.*, 2012) at the division plane during cytokinesis in one-cell embryos at 150 s after anaphase onset. At this time point, most control, but not *cyk-4(ts)*, embryos have
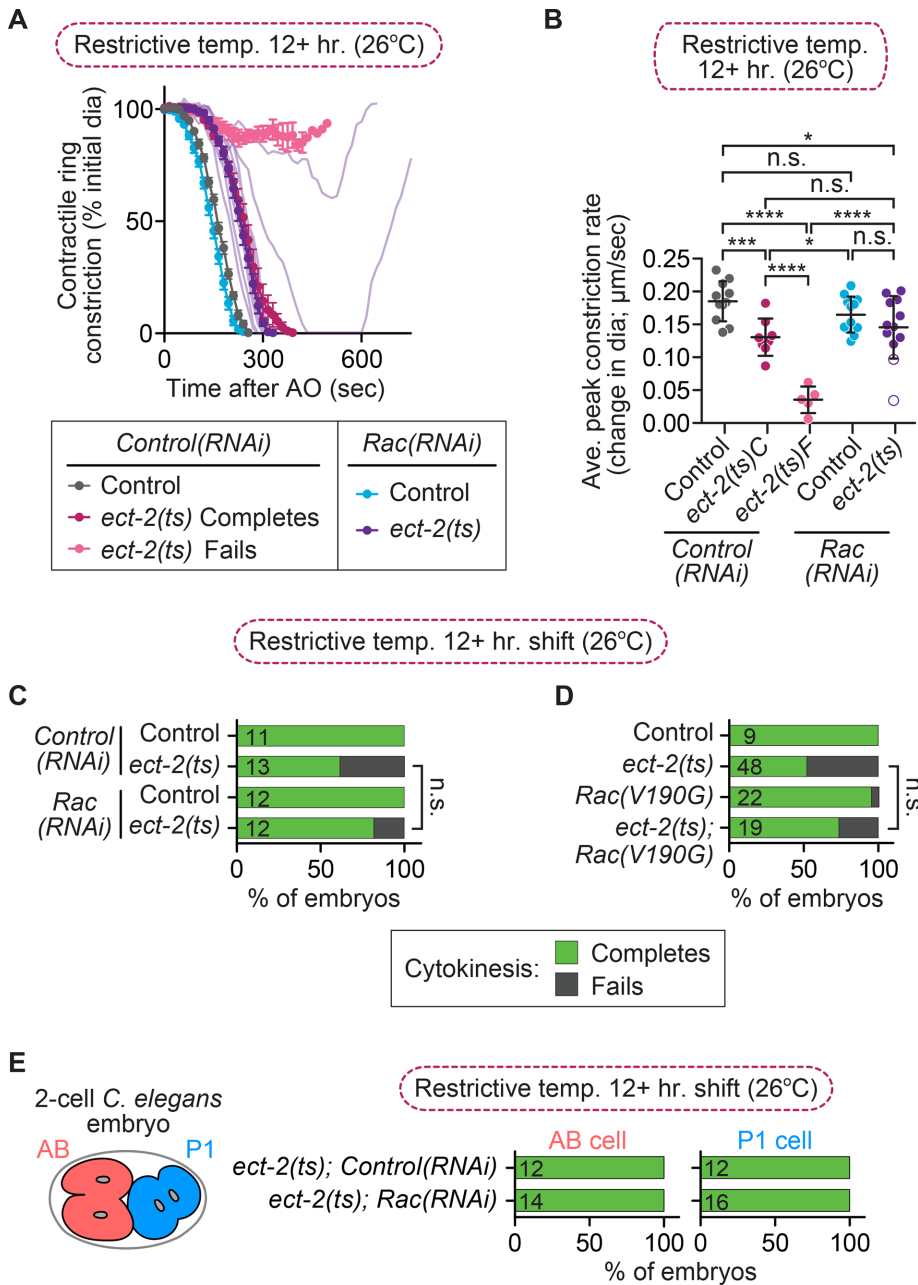
FIGURE 4: Rac disruption partially rescues cytokinesis failure in *ect-2(ts)* embryos. (A) Kinetic analysis of contractile ring constriction in control and *ect-2(ts)* mutant one-cell embryos at restrictive temperature (26°C) with and without *Rac(RNAi)*. Mean ring diameter vs. time, with all replicates for the *ect-2(ts); Rac(RNAi)* double mutant in a more transparent shade of deep purple. Error bars represent SEM. (B) Average rate of peak contractile ring constriction, plotted as the change in diameter (μm/s) for embryos in A. C, cytokinesis completes; F, cytokinesis fails. The white dots with a purple outline represent the *ect-2(ts); Rac(RNAi)* embryos that failed in cytokinesis. Error bars represent SD; *p* values were obtained by an unpaired, two-tailed Student's *t* test (Supplemental Table S3). (C) Cytokinesis failure and success rates for the embryos in A and (D) cytokinesis failure and success rates for one-cell embryos from *ect-2(ts)* mutant strains obtained from Loria *et al.* (2012). The number of embryos per genotype is indicated on each individual bar; *p* values were obtained by both Fisher's and Barnard's exact tests (Supplemental Table S3). (E) Schematic of the *C. elegans* two-cell embryo and graphs showing cytokinesis failure and success rates in the AB and P1 cell divisions for *ect-2(ts)* mutant embryos with or without *Rac(RNAi)*. n.s., *p* ≥ 0.05; **p* < 0.05; ****p* < 0.001; *****p* < 0.0001.

formed a double membrane at the furrow tip or initiated "furrow involution" (Lewellyn *et al.*, 2010; Supplemental Figure S1, A and B), as contractile rings in *cyk-4(ts)* embryos are less constricted

than in controls (Figure 1, A and C). We found no significant difference in the levels of GFP::myosin-II or GFP::Utr[ABD] at the division plane in *cyk-4(ts)* mutants relative to control embryos during this early stage of contractile ring constriction (Figure 5, A–C). Although in *cyk-4(ts)* embryos, contractile ring f-actin appeared to be less tightly bundled, likely due to the reduced constriction rate in *cyk-4(ts)* embryos relative to in controls (Figure 1, A and C), the total levels of f-actin at the division plane did not significantly differ from those in controls (Figure 5, B and D, and Supplemental Table S3). Thus the levels of f-actin and myosin-II, two downstream effectors of ECT-2 and Rho activation (Figure 1D and Supplemental Figure S2), are not significantly changed at the contractile ring upon functional disruption of CYK-4 GAP activity (unpaired Student's *t* test; Supplemental Table S3). This result suggests that CYK-4 is not upstream of ECT-2/Rho activation, but it does not exclude the possibility that ECT-2 is upstream of another function of CYK-4, such as modulation of Rac activity, or that CYK-4 may regulate another small GTPase (e.g., Cdc42).

The foregoing results, as well as the finding that we did not rescue the reduced rate of contractile ring constriction in *cyk-4(ts)* mutants by disrupting Rac activity (Figure 1C), could indicate a secondary positive role for CYK-4 or Rac during cytokinesis. In support of a possible positive role for Rac in cytokinesis, we saw a slight (although nonsignificant) enhancement of cytokinesis failure after depletion of Rac in both *formin(ts)* and *myosin-II(ts)* mutant embryos. However, Rac depletion on its own did not lead to any delays or obvious defects in cytokinesis in most of our experiments (Figures 1–4). In vitro, CYK-4 can also promote the GTP hydrolysis of Cdc42 (CDC-42 in *C. elegans*; hereafter, Cdc42; Toure *et al.*, 1998; Jantsch-Plunger *et al.*, 2000; Bastos *et al.*, 2012). Thus it is possible that CYK-4 GAP activity may also regulate Cdc42 during cell division. Depletion of Cdc42 by RNAi leads to a short but reproducible delay in the onset of contractile ring constriction (Jordan *et al.*, 2016). At this early stage of *C. elegans* development, Cdc42 plays an essential role in maintaining anterior–posterior polarity, which leads to asymmetric cell division and results in a larger anterior and smaller posterior blastomere (Gotta *et al.*, 2001; Kay and Hunter, 20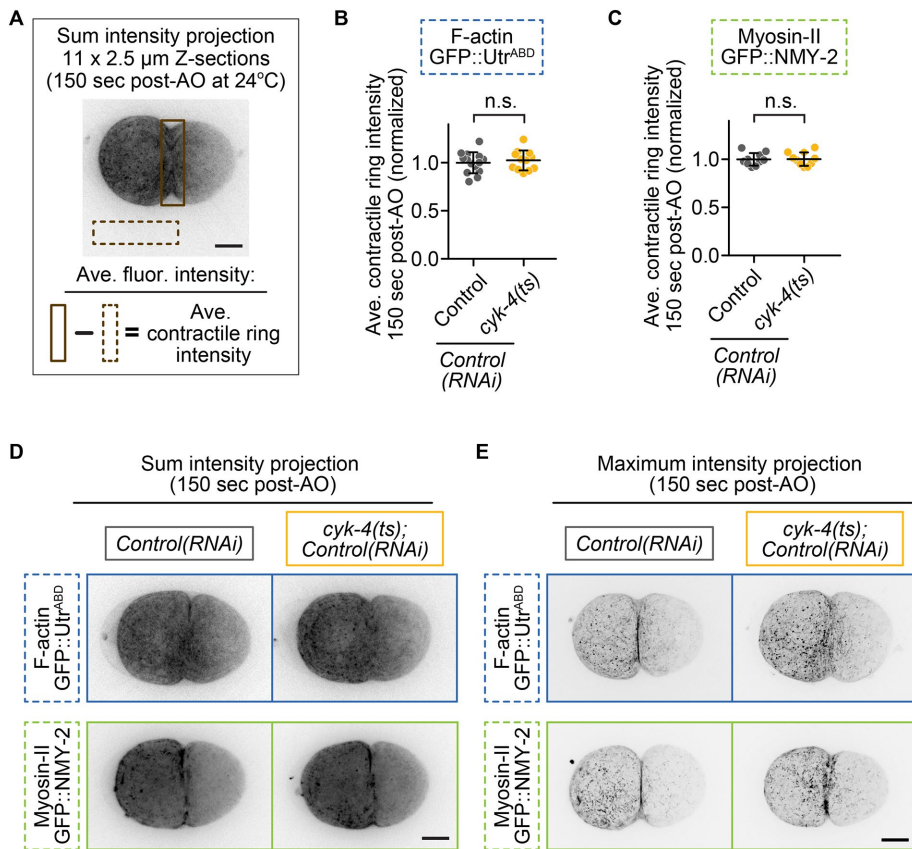01; Aceto *et al.*, 2006; Motegi and Sugimoto, 2006; Schonegg and Hyman, 2006). CYK-4 was also proposed to play a critical role in regulating cell polarity in the early embryo by functioning within the sperm to trigger polarity

FIGURE 5: Downstream targets of Rho, f-actin, and myosin-II are not reduced at the division plane in *cyk-4(ts)* mutants. (A) Schematic showing how quantitative image analysis was performed for B and C. (B, C) Quantification of contractile ring levels of (B) f-actin (GFP::Utr[ABD]) and (C) myosin-II (NMY-2::GFP) at 150 s post-AO at semirestrictive temperature (24°C). Error bars represent SD; *p* values were obtained by an unpaired, two-tailed Student's *t* test (Supplemental Table S3). (D) Representative sum projections of f-actin (GFP::Utr[ABD]) and myosin-II (NMY-2::GFP) in control and *cyk-4(ts)* embryos at 150 s post-AO. (E) Representative higher-*Z*-resolution maximum projections of f-actin and myosin-II at 150 s post-AO. Scale bars, 10 μm. n.s., *p* ≥ 0.05.

in control, *Rac(G60R)*, or *cyk-4(ts)* embryos, and, as expected, *cyk-4(ts); Rac(G60R); control(RNAi)* embryos failed in cytokinesis only 20% of the time (12 of 15 embryos divide; Figure 6, C and D, and Supplemental Table S3). In contrast, *cyk-4(ts); Rac(G60R); Cdc42(RNAi)* triple embryos failed in cytokinesis 100% of the time (0 of 11 embryos divide; Figure 6, C and D). Thus Cdc42 depletion significantly enhances the rate of cytokinesis failure relative to *cyk-4(ts); Rac(G60R); control(RNAi)* embryos (Fisher's and Barnard's exact tests; Supplemental Table S3), indicating that the rescue of cytokinesis failure in *cyk-4(ts)* mutants after Rac disruption is dependent on Cdc42. This is consistent with a role for CYK-4 in regulating Cdc42 during cytokinesis, although, due to the known role of Cdc42 and the PAR polarity proteins in cytokinesis (Jordan *et al.*, 2016) and lack of an effect of *Cdc42(RNAi)* on cytokinesis in the *cyk-4(ts)* mutant, it is difficult to draw any firm conclusions (Figure 6, C and D). In summary, our data support a model in which the predominant role for CYK-4's GAP activity during cytokinesis is to down-regulate Rac to allow for timely contractile ring constriction, at least in *C. elegans* one- and two-cell embryos (Supplemental Figure S2).

DISCUSSION

This work addressed the role of CYK-4 and the Rho-family small GTPase Rac in cytokinesis. Our results confirmed that, as was previously found, Rac inactivation partially rescued the rate of cytokinesis failure in a CYK-4 GAP mutant and a hypomorphic ECT-2 mutant (Canman *et al.*, 2008; Bastos *et al.*, 2012; Loria *et al.*, 2012; Cannet *et al.*, 2014; Zhang and Glotzer, 2015). However, we did not find evidence that Rac inhibition is a nonspecific "bypass" mechanism that generally facilitates contractile ring constriction, as was proposed by others (Loria *et al.*, 2012). Although Rac disruption did not rescue the rate of contractile ring constriction in *cyk-4(ts)* mutants, suggestive of another role for CYK-4 (or Rac) in cytokinesis, we did not find a role for CYK-4 upstream of ECT-2–mediated activation of Rho. We also did not find evidence that Rac activity changes the rate of or generally opposes contractile ring constriction; Rac inactivation did not rescue cytokinesis failure in strains with mutations in the Rho effectors diaphanous formin/CYK-1 and myosin-II/NMY-2. Furthermore, disrupting CYK-4 GAP activity did not affect the levels of f-actin or myosin-II in the contractile ring, indicating that CYK-4 is unlikely to act upstream of ECT-2–mediated activation of Rho. Our data instead suggest that CYK-4 negatively regulates Rac (and potentially Cdc42) during cytokinesis (Supplemental Figure S2).

There are at least three possible explanations for the mild rescue of ECT-2–mediated cytokinesis failure by loss of Rac: 1) Rac is a general suppressor of cytokinesis when the contractile ring is weakened, as was proposed (Loria *et al.*, 2012; Zhang and Glotzer, 2015), although our data showing a lack of rescue resulting from Rac disruption in *formin(ts)* and *myosin-II(ts)* mutants argue against this
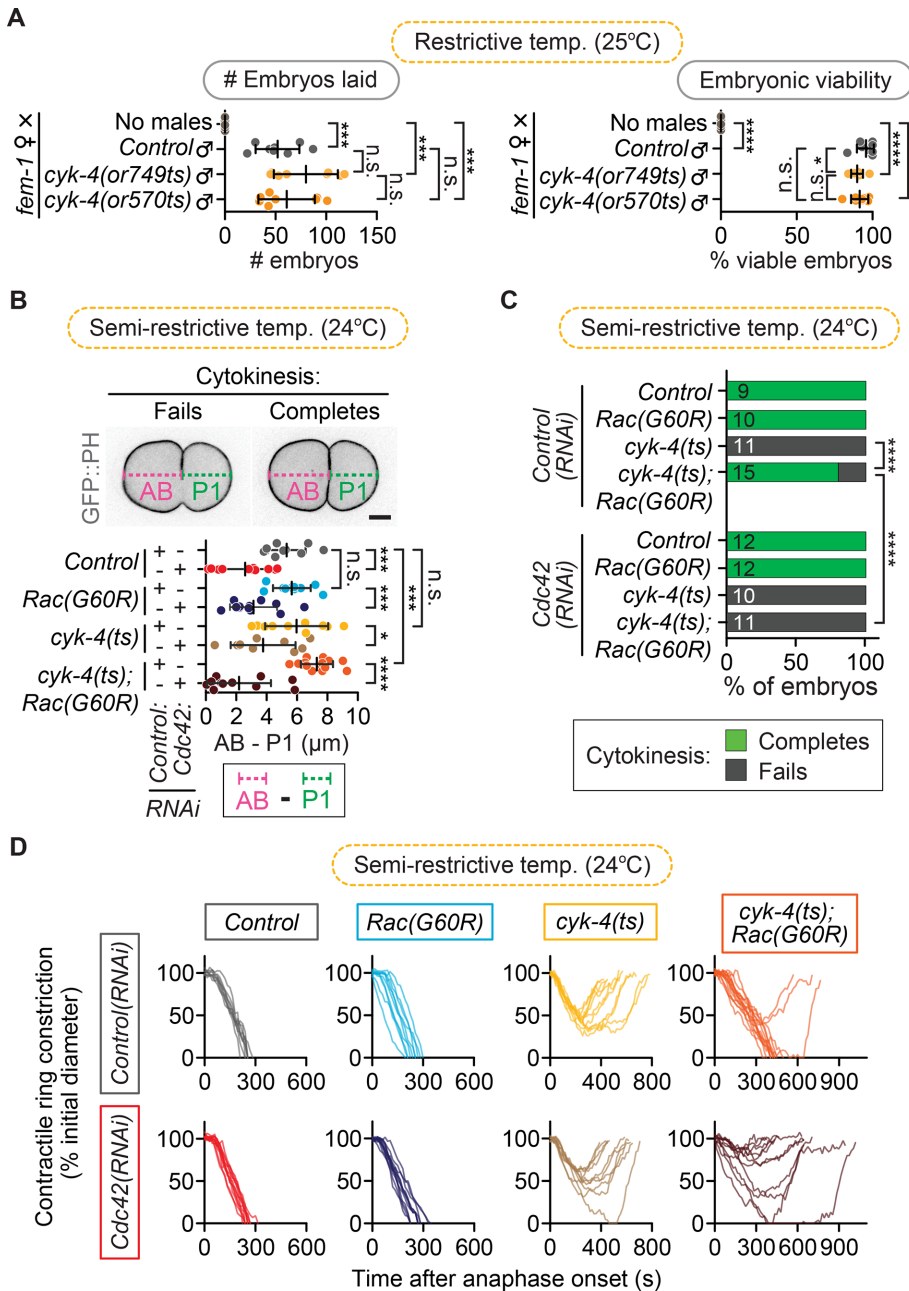
establishment upon fertilization (Jenkins *et al.*, 2006). However, we do not observe a dramatic increase in embryonic lethality or decrease in brood size when the sole sperm used for fertilization is homozygous for the *cyk-4(ts)* mutation, even at restrictive temperature, which would be expected if CYK-4 GAP activity plays this essential role in cell polarity (Figure 6A; unpaired Student's *t* test; Supplemental Table S3). Furthermore, we do not see a significant loss in the asymmetric position of the site of furrowing or daughter cell size in *cyk-4(ts)* single-mutant embryos (Figure 6B; unpaired Student's *t* test; Supplemental Table S3). Thus, if CYK-4 regulates Cdc42 in this system, it is likely not a major player in anterior–posterior cell polarity.

We recently identified a role for Cdc42 during cytokinesis in promoting the robustness of contractile ring constriction (Jordan *et al.*, 2016). One possibility is that CYK-4 regulates Cdc42 specifically during cytokinesis. We tested whether disrupting Cdc42 by RNAi could further rescue the rate of cytokinesis failure in one-cell *cyk-4(ts); Rac(lof)* double-mutant embryos. To ensure that we were able to obtain sufficient embryos from all genetic backgrounds, we used a partial Cdc42 depletion that reduced but did not eliminate cell polarity, as evidenced by the significant reduction in anterior-to-posterior daughter size asymmetry (Figure 6B; unpaired Student's *t* test; Supplemental Table S3). *Cdc42(RNAi)* did not significantly change the success rate or constriction kinetics of cytokinesis

FIGURE 6: *cyk-4(ts); Rac(G60R)* fail in cytokinesis when Cdc42 is depleted. (A) Paternal requirement test for sperm-supplied CYK-4 GAP activity in ~24- to 30-h brood size (left) and embryonic viability (right) when *cyk-4(ts)* males are mated with non–sperm-producing feminized *fem-1(hc17ts)* hermaphrodites at restrictive temperature (25°C). The low embryonic lethality rate indicates that sperm-supplied CYK-4 GAP activity is not essential to establish and/or maintain cell polarity. Error bars represent SD; *p* values were obtained by an unpaired, two-tailed Student's *t* test (Supplemental Table S3). (B) Asymmetry of furrow position in one-cell embryos (when cytokinesis fails) or of AB vs. P1 daughter cell size (when cytokinesis completes) among different genotypes used in D. Error bars represent SD; *p* values were obtained by an unpaired, two-tailed Student's *t* test (Supplemental Table S3). (C) Cytokinesis failure and success rates for different genotypes in D. The number of embryos per genotype is indicated on each individual bar; *p* values were obtained by both Fisher's and Barnard's exact tests (Supplemental Table S3). (D) Kinetic analysis of contractile ring constriction in control, *cyk-4(ts)*, *Rac(G60R)*, and *cyk-4(ts); Rac(G60R)* double-mutant one-cell embryos with and without *Cdc42(RNAi)* at semirestrictive temperature (24°C). Embryos from each genotype are plotted on individual graphs to make it easier to see, and traces for all individual embryos are shown. Scale bar, 10 μm. n.s., *p* > 0.05; *p < 0.05; ***p < 0.001; ****p < 0.0001.

model; 2) Rac and Rho are mutually inhibitory and/or compete for binding partners (e.g., RhoGDIs, GEFs, GAPs, or effectors), so that perturbing Rac activity promotes more Rho activity, as can occur in other cell contexts (e.g., Machacek *et al.*, 2009; Boulter *et al.*, 2010; Garcia-Mata *et al.*, 2011); or 3) the GEF activity of ECT-2 promotes Rac activation during cytokinesis either directly or via CYK-4 (Supplemental Figure S2), which is inhibitory to contractile ring constriction. In vitro, ECT-2 was found in one study to be an even more potent GEF for Rac and Cdc42 than Rho (Tatsumoto *et al.*, 1999); therefore this is indeed a possibility. This would explain why disruption of Rac activity can rescue cytokinesis failure in both *cyk-4(ts)* and, to some extent, *ect-2(ts)* mutant embryos but not *formin(ts)* or *myosin-II(ts)* embryos. Thus we propose that, in addition to its positive role in cytokinesis via Rho activation, ECT-2 (alone or through CYK-4) may function in a negative regulatory feedback loop to spatiotemporally control Rac activity and/or GTPase flux during cytokinesis (Supplemental Figure S2).

Our results on Rho-effector levels in the contractile ring after CYK-4 disruption conflict with the results reported by Loria *et al.* (2012) but agree with previous analyses of the effect of CYK-4/Centralspindlin disruption on myosin-II targeting to the contractile ring during ring constriction (Canman *et al.*, 2008; Lewellyn *et al.*, 2011), including myosin-II analysis presented more recently by the same lab that published the Loria *et al.* (2012) work (Zhang and Glotzer, 2015). One possible difference between these studies is the method used to quantify fluorescence intensity in the contractile ring. Loria *et al.* (2012) quantified the levels within a region of interest (ROI) around the division plane from the maximum projected images of 5 × 2.5 μm central Z-sections, applied a threshold with a minimal value of 1.25 times the background intensity, and then integrated and normalized to the background. Here we quantified the signal in a ROI around the entire division plane from the sum-projected images from 11 × 2.5 μm Z-sections, subtracted the sum-projected background signal from an identical-sized ROI, and then normalized to the levels in control embryos (Figure 5). Although our analysis reflects all of the GFP signal in the contractile ring, the arbitrary thresholding and maximum projections used in the other analysis would decrease detection of more diffuse cytoskeletal signal in the contractile ring. In the case of *cyk-4(ts)* mutants, a more diffuse signal

would be expected due to the reduced rate of contractile ring constriction (Figure 1C) and thus likely reduced rate of actomyosin bundling. Furthermore, limiting analysis to only 5 × 2.5 μm central Z-sections during imaging (Loria et al., 2012; vs. 11 × 2.5 μm here; C. elegans embryos are ~25–30 μm in diameter) would be more likely to miss regions of the equatorial cell cortex that contain peak levels of contractile ring proteins especially early in cytokinesis, as contractile ring constriction itself is asymmetric in this system and initiates from a single position along the equatorial cell cortex (Maddox et al., 2007).

We also found that rescue of cyk-4(ts) GAP-defective mutants by Rac depletion is Cdc42 dependent. This could represent a role for CYK-4 in regulating Cdc42 activity during cell polarity maintenance and/or cytokinesis or general Rho-family imbalance due to Cdc42-mediated competition for inhibitory Rho-family effectors and/or regulators (e.g., GDIs; Tatsumoto et al., 1999; Machacek et al., 2009; Boulter et al., 2010; Garcia-Mata et al., 2011). Cdc42 hyperactivation was found to inhibit the formation of a focused band of f-actin in the contractile ring in HeLa cells (Zhu et al., 2011), and yet depletion of Cdc42 does not block contractile ring constriction in HeLa cells or C. elegans embryos (Zhu et al., 2011; Jordan et al., 2016). In the early C. elegans embryo, Cdc42 plays an important role in maintaining anterior–posterior (AP) polarity (Gotta et al., 2001; Kay and Hunter, 2001), and we recently identified a role for Cdc42 (via a collaboration with the PAR polarity proteins) in promoting f-actin accumulation in the contractile ring (Jordan et al., 2016). Thus it is possible that CYK-4 may regulate this function of Cdc42 during polarity maintenance. Sperm-supplied CYK-4 has also been implicated in regulating AP cell polarity in C. elegans embryos (Jenkins et al., 2006), but we see either no difference or only a mildly significant difference in embryonic lethality and no significant difference in brood size when homozygous cyk-4(ts) males are mated with genetically feminized worms (fem-1 mutant) at restrictive temperature, as would be expected if AP polarity was grossly disrupted. Furthermore, in cyk-4(ts) single mutants, we do not see a change in two strong indicators of a polarity disruption: 1) asymmetric cleavage furrow position along the AP axis and 2) daughter size asymmetry (Figure 6B). We do, however, see a significantly more posteriorized furrow position in cyk-4(ts); Rac(lof) double mutants (Figure 6). This is a similar phenotype to that seen after depletion of the Cdc42 GAP chimaerin 1, known to be a regulator of Cdc42 during cell polarity maintenance in this system (Kumfer et al., 2010; Beatty et al., 2013). Nevertheless, enhancement of cytokinesis failure alone cannot confirm a role for CYK-4 in Cdc42 regulation during contractile ring constriction. Taken together, our data support a model in which, at least in the early C. elegans embryo, CYK-4 functions to inhibit Rac activity and does not participate directly in Rho activation (Supplemental Figure S2).

MATERIALS AND METHODS
Strain maintenance
C. elegans were kept on standard Nematode Growth Medium (NGM) plates seeded with OP50 Escherichia coli bacteria as described (Brenner, 1974). All strain names and genotypes used in this study are listed in Supplemental Table S1.

Temperature control
All control and ts strains were raised in an incubator (Binder) kept at permissive temperature (16 ± 0.5°C), and all fast-acting ts strains were also dissected in cooled (~16°C) M9 buffer (3 g of KH_2PO_4, 6 g of Na_2HPO_4, 5 g of NaCl, 1 ml of 1 M $MgSO_4$, and H_2O to 1 l and sterilized by autoclaving) until just before the one- or two-cell

division. For the non–fast-acting ect-2(ts) experiments (Figure 4), worms were raised at permissive temperature (16°C) until the L4 stage, at which time they were moved to a 26°C incubator (Binder) overnight for at least 12 h and dissected in a warmed room (~26°C) in ~26°C M9 buffer (Brenner, 1974).

Live-cell imaging was performed in a thermally controlled room. Room temperature was monitored with two thermometers attached directly to the objective and another thermometer attached to the stage via a glue gun to monitor the temperature of the specimen during filming. Wherever mentioned, experimental temperatures were calculated by averaging the values from the two thermometers attached to the objective and were as follows: cyk-4(ts) semirestrictive (24.0 ± 0.5°C); ect-2(ts) restrictive (26.0 ± 0.5°C); formin(ts) semipermissive (18.5 ± 0.5°C); formin(ts) semirestrictive (23.5 ± 0.5°C); myosin-II(ts) semipermissive (22.5 ± 0.5°C); and myosin-II(ts) semirestrictive (25.5 ± 0.5°C). Temperatures are defined for each individual mutant allele as follows: permissive temperature, all ts embryos complete cytokinesis with kinetics most similar to non-ts controls; semipermissive temperature, highest temperature at which all ts embryos complete cytokinesis; semirestrictive temperature, lowest temperature at which all ts embryos fail in cytokinesis; and restrictive temperature, all embryos fail in cytokinesis with a null-like phenotype (aside from the ect-2(ts) mutant, which often divides successfully even at the restrictive temperature of 26°C).

Live-cell imaging
Single-cell embryos were mounted on a 2% agar pad as described previously (Gonczy et al., 1999; Jordan et al., 2016). Imaging was performed on a Nikon Ti inverted microscope with 40×/1.3 numerical aperture (NA) and 60×/1.4 NA oil-immersion PlanApochromat objectives using a Yokagawa CSU-10 spinning-disk confocal equipped with Borealis (Spectral Applied Research) and a Hamamatsu Orca ER camera. Z-sectioning was done with a piezo-driven motorized stage (Applied Scientific Instrumentation), and focus was maintained using Perfect Focus (Nikon) before each Z-series acquisition. Solid-state 150-mW lasers were used for excitation at 488 and 561 nm for enhanced GFP and mCherry, respectively (Spectral Applied Research), and a filter wheel was used for emission wavelength selection (Sutter Instruments). The imaging system was controlled by MetaMorph software (Molecular Devices).

A central, transmitted light image and through-cell GFP and mCherry fluorescent Z-series were collected every 15 or 30 s to measure ingression kinetics (see later description). For data presented in Figures 1–4 and 6 and Supplemental Figure S1, embryos were imaged with the 40×/1.3 NA oil objective with 2 × 2 binning and 100-ms exposures. Laser power was tuned to 20% for the 488-nm laser and 50% for the 561-nm laser (except for Figure 6, B–D, where we looked at the effect of Cdc42(RNAi) on cytokinesis in cyk-4(ts) embryos with and without Rac(G60R); the 561-nm laser intensity was 70%). For data presented in Figures 1, 3, and 4 (cyk-4(ts) kinetics with and without Rac(G60R) or Rac(RNAi); cyk-1(ts) kinetics with and without Rac(G60R); and nmy-2(ts) kinetics with and without Rac(G60R)), the same imaging parameters were used, except that embryos were imaged every 30 s. The Z-sectioning was as follows: 13 × 2 μm steps (Figures 1–4 and 6, B–D, and Supplemental Figure S1C), with the exception of a few embryos filmed using 7 × 2 μm steps in Figures 2 and 3 at the semirestrictive temperature, where the contractile ring closes in the central Z-plane. The embryos imaged using 7 × 2 μm steps were acquired with the 60×/1.4 NA oil objective 2 × 2 binning (Figures 2 and 3). For analysis of the contractile ring levels of GFP::NMY-2 (Munro et al., 2004) and GFP::Utr[ABD], a reporter for f-actin (Burkel et al., 2007; Tse et al., 2012), a single

11 × 2.5 µm or 65 × 0.5 µm Z-section image stack (see also *Image analysis* section) was taken 150 s after AO using a 60×/1.4 NA oil-immersion PlanApochromat objective with 2 × 2 binning on a Hamamatsu Orca ER camera and 150-mW, 488- and 561-nm lasers at 50% laser power intensity with 100-ms exposures (Figure 5).

Image analysis

MetaMorph (Molecular Devices) and FIJI (ImageJ [Schindelin *et al.*, 2012; Schneider *et al.*, 2012]) software were used for all data analysis. Contractile ring constriction was measured from the time of metaphase (time point immediately before AO) until AO of the next division, or, in the case of cytokinesis failure, until complete contractile ring regression. The contractile ring diameter was measured at each time point in the Z-section where the ring was most open and displayed as a percentage of the initial diameter over time. The rate of ingression is plotted as micrometers/second when the rate of ingression peaks from ~90–50% of the initial cell diameter. When embryos did not ingress to 50% of the initial cell diameter, the point of deepest contractile ring constriction was used (Figures 1–4). Where histone markers were not available (in strains with *Rac(lof)* and *cyk-4(ts);GFP::NMY-2*), AO was determined by transmitted light.

The levels of f-actin and myosin-II (GFP::Utr^ABD and GFP::NMY-2) in the contractile ring in *cyk-4(ts)* embryos (at semirestrictive temperature, 24°C) were calculated as follows. All 11 × 2.5 µm Z-stacks were sum projected using FIJI (Figure 5, B–D). A region of fixed size (195 × 38 pixels) surrounding the entire division plane was used to measure the average pixel intensity, and measurements from a region of the same size in a nearby background area, outside of the embryo, were subtracted for each individual embryo, as schematized in Figure 5A. These data were normalized to controls and plotted as the average intensity at 150-s post-AO (Figure 5, B–D). Where higher-resolution images are shown (Figure 5E), a 65 × 0.5 µm Z-section stack acquired at 150 s post-AO and a maximum projection image for all 65 Z-sections were generated using FIJI.

The asymmetric differences in daughter cell size were calculated by measuring the length of the newly formed AB (anterior) and P1 (posterior) blastomeres using the time point immediately after completion of cytokinesis (Figure 6B, showing *cyk-4(ts)* with and without *Rac(G60R)* and *Cdc42(RNAi)*). The length of the posterior P1 cell was subtracted from the length of the anterior AB cell. Cell size measurement was done using a single central plane from the 488-nm GFP channel. When embryos failed to complete cytokinesis, a similar measurement was taken using the distance from the anterior and posterior poles to the cleavage furrow at the time of maximum contractile ring constriction. Analysis of the time from AO to double-membrane formation in Supplemental Figure S1 was done using the same embryos as in Figure 1A (kinetics of cytokinesis in *cyk-4(ts)* mutant embryos with and without *Rac(RNAi)*).

Embryonic viability and brood size

The *fem-1(hc17ts)* hermaphrodites were raised at 25°C to feminize them (by blocking sperm production) and then singled as L4s onto individual mating plates (35-mm NGM agar plates seeded with 10 µl of OP50; Brenner, 1974). The *cyk-4(ts)* males were also raised at 25°C from the ~L3/L4 stage. Seven males per genotype (except for the no-male controls) were added to each plate containing a single hermaphrodite and allowed to mate for ~15 h at 25°C. To ensure that the *fem-1(hc17ts)* hermaphrodites were feminized (and thus sterile), we did not add males to one set of *fem-1(ts)* hermaphrodites (no-male controls). The adults from each individual cross were transferred twice to a new plate every ~10 h (after laying ~50 embryos). The numbers of viable progeny and dead embryos per

feminized hermaphrodite (Figure 6A) were quantified for two plates per cross (representing ~24–30 h of egg laying) at 24 h after transferring off the adults (to allow all embryos to hatch) using a digital counting pen (Fisher) on a Nikon dissecting microscope.

Feeding RNAi

All primers and DNA template used for RNAi experiments are listed in Supplemental Table S2. Cloning was performed by inserting the *Rac/ced-10* sequence into the L4440 vector using standard cloning protocols and then transformed into HT115 *E. coli* (Timmons *et al.*, 2001). The empty L4440 vector in HT115 cells was used as a control. RNAi feeding bacteria were inoculated in Luria broth with 100 µg/ml ampicillin for either 7 h at 37°C or 16 h at 32°C. A 300-µl amount of this culture was plated on RNAi plates (NGM agar plates [Brenner, 1974] supplemented with 50 µg/ml ampicillin and 1 mM isopropyl-β-D-thiogalactoside). After drying, the plates were grown at 32°C for 24–48 h. L1 worms were transferred onto RNAi plates and then grown at 16°C until young adulthood, when they were dissected to obtain the embryos. RNAi knockdown for *Rac/ced-10* was confirmed by observing 1) deeper furrowing during pseudocleavage and 2) completion of cytokinesis in *cyk-4(ts)* mutant embryos at the semirestrictive temperature (24 ± 0.5°C). Cdc42 (CDC-42) knockdown was confirmed by assaying embryonic lethality and loss of cell division asymmetry (Figure 6B).

Statistical analysis

Unpaired Student's *t* tests were conducted using GraphPad Prism software. n.s., $p \geq 0.05$; *$p < 0.05$; **$p < 0.01$; ***$p < 0.001$; and ****$p < 0.0001$. Error bars for traces of cell diameter over time during cytokinesis represent SEM. Error bars for contractile ring constriction rates, myosin-II and f-actin levels, embryonic lethality, brood size, and asymmetry of furrow position represent SD. Statistics for cytokinesis completion/failure bar graphs used a two-tailed Fisher's exact test, but this analysis was also done with a Barnard's exact test (Supplemental Table S3). See also statistical analysis in Supplemental Table S3 for all *p* values.

REFERENCES

Aceto D, Beers M, Kemphues KJ (2006). Interaction of PAR-6 with CDC-42 is required for maintenance but not establishment of PAR asymmetry in C. elegans. Dev Biol 299, 386–397.

Bastos RN, Penate X, Bates M, Hammond D, Barr FA (2012). CYK4 inhibits Rac1-dependent PAK1 and ARHGEF7 effector pathways during cytokinesis. J Cell Biol 198, 865–880.

Beatty A, Morton DG, Kemphues K (2013). PAR-2, LGL-1 and the CDC-42 GAP CHIN-1 act in distinct pathways to maintain polarity in the C. elegans embryo. Development 140, 2005–2014.

Bement WM, Benink HA, von Dassow G (2005). A microtubule-dependent zone of active RhoA during cleavage plane specification. J Cell Biol 170, 91–101.

Boulter E, Garcia-Mata R, Guilluy C, Dubash A, Rossi G, Brennwald PJ, Burridge K (2010). Regulation of Rho GTPase crosstalk, degradation and activity by RhoGDI1. Nat Cell Biol 12, 477–483.

Brenner S (1974). The genetics of Caenorhabditis elegans. Genetics 77, 71–94.

Burkard ME, Maciejowski J, Rodriguez-Bravo V, Repka M, Lowery DM, Clauser KR, Zhang C, Shokat KM, Carr SA, Yaffe MB, Jallepalli PV (2009). Plk1 self-organization and priming phosphorylation of HsCYK-4 at the spindle midzone regulate the onset of division in human cells. PLoS Biol 7, e1000111.

Burkel BM, von Dassow G, Bement WM (2007). Versatile fluorescent probes for actin filaments based on the actin-binding domain of utrophin. Cell Motil Cytoskeleton 64, 822–832.

Cabello J, Samann J, Gomez-Orte E, Erazo T, Coppa A, Pujol A, Bussing I, Schulze B, Lizcano JM, Ferrer I, et al. (2014). PDR-1/hParkin negatively regulates the phagocytosis of apoptotic cell corpses in Caenorhabditis elegans. Cell Death Dis 5, e1120.

Canman JC, Lewellyn L, Laband K, Smerdon SJ, Desai A, Bowerman B, Oegema K (2008). Inhibition of Rac by the GAP activity of centralspindlin is essential for cytokinesis. Science 322, 1543–1546.

Cannet A, Schmidt S, Delaval B, Debant A (2014). Identification of a mitotic Rac-GEF, Trio, that counteracts MgcRacGAP function during cytokinesis. Mol Biol Cell 25, 4063–4071.

Davies T, Jordan SN, Chand V, Sees JA, Laband K, Carvalho AX, Shirasu-Hiza M, Kovar DR, Dumont J, Canman JC (2014). High-resolution temporal analysis reveals a functional timeline for the molecular regulation of cytokinesis. Dev Cell 30, 209–223.

D'Avino PP, Giansanti MG, Petronczki M (2015). Cytokinesis in animal cells. Cold Spring Harb Perspect Biol 7, a015834.

D'Avino PP, Savoian MS, Glover DM (2004). Mutations in sticky lead to defective organization of the contractile ring during cytokinesis and are enhanced by Rho and suppressed by Rac. J Cell Biol 166, 61–71.

Drechsel DN, Hyman AA, Hall A, Glotzer M (1997). A requirement for Rho and Cdc42 during cytokinesis in Xenopus embryos. Curr Biol 7, 12–23.

Garcia-Mata R, Boulter E, Burridge K (2011). The 'invisible hand': regulation of RHO GTPases by RHOGDIs. Nat Rev Mol Cell Biol 12, 493–504.

Goldstein AY, Jan YN, Luo L (2005). Function and regulation of Tumbleweed (RacGAP50C) in neuroblast proliferation and neuronal morphogenesis. Proc Natl Acad Sci USA 102, 3834–3839.

Gonczy P, Schnabel H, Kaletta T, Amores AD, Hyman T, Schnabel R (1999). Dissection of cell division processes in the one cell stage Caenorhabditis elegans embryo by mutational analysis. J Cell Biol 144, 927–946.

Gotta M, Abraham MC, Ahringer J (2001). CDC-42 controls early cell polarity and spindle orientation in C. elegans. Curr Biol 11, 482–488.

Green RA, Paluch E, Oegema K (2012). Cytokinesis in animal cells. Annu Rev Cell Dev Biol 28, 29–58.

Gremer L, Merbitz-Zahradnik T, Dvorsky R, Cirstea IC, Kratz CP, Zenker M, Wittinghofer A, Ahmadian MR (2011). Germline KRAS mutations cause aberrant biochemical and physical properties leading to developmental disorders. Hum Mutat 32, 33–43.

Hall A (2012). Rho family GTPases. Biochem Soc Trans 40, 1378–1382.

Hirose K, Kawashima T, Iwamoto I, Nosaka T, Kitamura T (2001). MgcRacGAP is involved in cytokinesis through associating with mitotic spindle and midbody. J Biol Chem 276, 5821–5828.

Jantsch-Plunger V, Gonczy P, Romano A, Schnabel H, Hamill D, Schnabel R, Hyman AA, Glotzer M (2000). CYK-4: A Rho family gtpase activating protein (GAP) required for central spindle formation and cytokinesis. J Cell Biol 149, 1391–1404.

Jenkins N, Saam JR, Mango SE (2006). CYK-4/GAP provides a localized cue to initiate anteroposterior polarity upon fertilization. Science 313, 1298–1301.

Jordan SN, Canman JC (2012). Rho GTPases in animal cell cytokinesis: an occupation by the one percent. Cytoskeleton (Hoboken) 69, 919–930.

Jordan SN, Davies T, Zhuravlev Y, Dumont J, Shirasu-Hiza M, Canman JC (2016). Cortical PAR polarity proteins promote robust cytokinesis during asymmetric cell division. J Cell Biol 212, 39–49.

Kamijo K, Ohara N, Abe M, Uchimura T, Hosoya H, Lee JS, Miki T (2006). Dissecting the role of Rho-mediated signaling in contractile ring formation. Mol Biol Cell 17, 43–55.

Kay AJ, Hunter CP (2001). CDC-42 regulates PAR protein localization and function to control cellular and embryonic polarity in C. elegans. Curr Biol 11, 474–481.

Kim H, Guo F, Brahma S, Xing Y, Burkard ME (2014). Centralspindlin assembly and 2 phosphorylations on MgcRacGAP by Polo-like kinase 1 initiate Ect2 binding in early cytokinesis. Cell Cycle 13, 2952–2961.

Kimura K, Tsuji T, Takada Y, Miki T, Narumiya S (2000). Accumulation of GTP-bound RhoA during cytokinesis and a critical role of ECT2 in this accumulation. J Biol Chem 275, 17233–17236.

Kinsella BT, Erdman RA, Maltese WA (1991). Carboxyl-terminal isoprenylation of ras-related GTP-binding proteins encoded by rac1, rac2, and ralA. J Biol Chem 266, 9786–9794.

Kumfer KT, Cook SJ, Squirrell JM, Eliceiri KW, Peel N, O'Connell KF, White JG (2010). CGEF-1 and CHIN-1 regulate CDC-42 activity during asymmetric division in the Caenorhabditis elegans embryo. Mol Biol Cell 21, 266–277.

Lewellyn L, Carvalho A, Desai A, Maddox AS, Oegema K (2011). The chromosomal passenger complex and centralspindlin independently contribute to contractile ring assembly. J Cell Biol 193, 155–169.

Lewellyn L, Dumont J, Desai A, Oegema K (2010). Analyzing the effects of delaying aster separation on furrow formation during cytokinesis in the Caenorhabditis elegans embryo. Mol Biol Cell 21, 50–62.

Liu J, Maduzia LL, Shirayama M, Mello CC (2010). NMY-2 maintains cellular asymmetry and cell boundaries, and promotes a SRC-dependent asymmetric cell division. Dev Biol 339, 366–373.

Loria A, Longhini KM, Glotzer M (2012). The RhoGAP domain of CYK-4 has an essential role in RhoA activation. Curr Biol 22, 213–219.

Ma C, Benink HA, Cheng D, Montplaisir V, Wang L, Xi Y, Zheng PP, Bement WM, Liu XJ (2006). Cdc42 activation couples spindle positioning to first polar body formation in oocyte maturation. Curr Biol 16, 214–220.

Machacek M, Hodgson L, Welch C, Elliott H, Pertz O, Nalbant P, Abell A, Johnson GL, Hahn KM, Danuser G (2009). Coordination of Rho GTPase activities during cell protrusion. Nature 461, 99–103.

Maddox AS, Lewellyn L, Desai A, Oegema K (2007). Anillin and the septins promote asymmetric ingression of the cytokinetic furrow. Dev Cell 12, 827–835.

Mao Y, Finnemann SC (2015). Regulation of phagocytosis by Rho GTPases. Small GTPases 6, 89–99.

Miller AL, Bement WM (2009). Regulation of cytokinesis by Rho GTPase flux. Nat Cell Biol 11, 71–77.

Mishima M, Kaitna S, Glotzer M (2002). Central spindle assembly and cytokinesis require a kinesin-like protein/RhoGAP complex with microtubule bundling activity. Dev Cell 2, 41–54.

Motegi F, Sugimoto A (2006). Sequential functioning of the ECT-2 RhoGEF, RHO-1 and CDC-42 establishes cell polarity in Caenorhabditis elegans embryos. Nat Cell Biol 8, 978–985.

Munro E, Nance J, Priess JR (2004). Cortical flows powered by asymmetrical contraction transport PAR proteins to establish and maintain anterior-posterior polarity in the early C. elegans embryo. Dev Cell 7, 413–424.

O'Connell CB, Wheatley SP, Ahmed S, Wang YL (1999). The small GTP-binding protein rho regulates cortical activities in cultured cells during division. J Cell Biol 144, 305–313.

Pavicic-Kaltenbrunner V, Mishima M, Glotzer M (2007). Cooperative assembly of CYK-4/MgcRacGAP and ZEN-4/MKLP1 to form the centralspindlin complex. Mol Biol Cell 18, 4992–5003.

Pollard TD (2010). Mechanics of cytokinesis in eukaryotes. Curr Opin Cell Biol 22, 50–56.

Reddien PW, Horvitz HR (2000). CED-2/CrkII and CED-10/Rac control phagocytosis and cell migration in Caenorhabditis elegans. Nat Cell Biol 2, 131–136.

Ridley AJ (2015). Rho GTPase signalling in cell migration. Curr Opin Cell Biol 36, 103–112.

Roberts PJ, Mitin N, Keller PJ, Chenette EJ, Madigan JP, Currin RO, Cox AD, Wilson O, Kirschmeier P, Der CJ (2008). Rho family GTPase modification and dependence on CAAX motif-signaled posttranslational modification. J Biol Chem 283, 25150–25163.

Schindelin J, Arganda-Carreras I, Frise E, Kaynig V, Longair M, Pietzsch T, Preibisch S, Rueden C, Saalfeld S, Schmid B, et al. (2012). Fiji: an open-source platform for biological-image analysis. Nat Methods 9, 676–682.

Schneider CA, Rasband WS, Eliceiri KW (2012). NIH Image to ImageJ: 25 years of image analysis. Nat Methods 9, 671–675.

Schonegg S, Hyman AA (2006). CDC-42 and RHO-1 coordinate acto-myosin contractility and PAR protein localization during polarity establishment in C. elegans embryos. Development 133, 3507–3516.

Shakir MA, Gill JS, Lundquist EA (2006). Interactions of UNC-34 enabled with Rac GTPases and the NIK kinase MIG-15 in Caenorhabditis elegans axon pathfinding and neuronal migration. Genetics 172, 893–913.

Somers WG, Saint R (2003). A RhoGEF and Rho family GTPase-activating protein complex links the contractile ring to cortical microtubules at the onset of cytokinesis. Dev Cell 4, 29–39.

Steffen A, Ladwein M, Dimchev GA, Hein A, Schwenkmezger L, Arens S, Ladwein KI, Margit Holleboom J, Schur F, Victor Small J, et al. (2013). Rac function is crucial for cell migration but is not required for spreading and focal adhesion formation. J Cell Sci 126, 4572–4588.

Sun L, Liu O, Desai J, Karbassi F, Sylvain MA, Shi A, Rocheleau CE, Grant BD (2012). CED-10/Rac1 regulates endocytic recycling through the RAB-5 GAP TBC-2. PLoS Genet 8, e1002785.

Tatsumoto T, Xie X, Blumenthal R, Okamoto I, Miki T (1999). Human ECT2 is an exchange factor for Rho GTPases, phosphorylated in G2/M phases, and involved in cytokinesis. J Cell Biol 147, 921–928.

Timmons L, Court DL, Fire A (2001). Ingestion of bacterially expressed dsRNAs can produce specific and potent genetic interference in Caenorhabditis elegans. Gene 263, 103–112.

Toure A, Dorseuil O, Morin L, Timmons P, Jegou B, Reibel L, Gacon G (1998). MgcRacGAP, a new human GTPase-activating protein for Rac and Cdc42 similar to Drosophila rotundRacGAP gene product, is expressed in male germ cells. J Biol Chem 273, 6019–6023.

Tse YC, Werner M, Longhini KM, Labbe JC, Goldstein B, Glotzer M (2012). RhoA activation during polarization and cytokinesis of the early Caenorhabditis elegans embryo is differentially dependent on NOP-1 and CYK-4. Mol Biol Cell 23, 4020–4031.

Wang ZB, Jiang ZZ, Zhang QH, Hu MW, Huang L, Ou XH, Guo L, Ouyang YC, Hou Y, Brakebusch C, et al. (2013). Specific deletion of Cdc42 does not affect meiotic spindle organization/migration and homologous chromosome segregation but disrupts polarity establishment and cytokinesis in mouse oocytes. Mol Biol Cell 24, 3832–3841.

Wolfe BA, Takaki T, Petronczki M, Glotzer M (2009). Polo-like kinase 1 directs assembly of the HsCyk-4 RhoGAP/Ect2 RhoGEF complex to initiate cleavage furrow formation. PLoS Biol 7, e1000110.

Yoshizaki H, Ohba Y, Parrini MC, Dulyaninova NG, Bresnick AR, Mochizuki N, Matsuda M (2004). Cell type-specific regulation of RhoA activity during cytokinesis. J Biol Chem 279, 44756–44762.

Yuce O, Piekny A, Glotzer M (2005). An ECT2-centralspindlin complex regulates the localization and function of RhoA. J Cell Biol 170, 571–582.

Zanin E, Desai A, Poser I, Toyoda Y, Andree C, Moebius C, Bickle M, Conradt B, Piekny A, Oegema K (2013). A conserved RhoGAP limits M phase contractility and coordinates with microtubule asters to confine RhoA during cytokinesis. Dev Cell 26, 496–510.

Zhang D, Glotzer M (2015). The RhoGAP activity of CYK-4/MgcRacGAP functions non-canonically by promoting RhoA activation during cytokinesis. Elife 4, doi: 10.7554/eLife.08898.

Zhang W, Robinson DN (2005). Balance of actively generated contractile and resistive forces controls cytokinesis dynamics. Proc Natl Acad Sci USA 102, 7186–7191.

Zhang X, Ma C, Miller AL, Katbi HA, Bement WM, Liu XJ (2008). Polar body emission requires a RhoA contractile ring and Cdc42-mediated membrane protrusion. Dev Cell 15, 386–400.

Zhao WM, Fang G (2005). MgcRacGAP controls the assembly of the contractile ring and the initiation of cytokinesis. Proc Natl Acad Sci USA 102, 13158–13163.

Zhu X, Wang J, Moriguchi K, Liow LT, Ahmed S, Kaverina I, Murata-Hori M (2011). Proper regulation of Cdc42 activity is required for tight actin concentration at the equator during cytokinesis in adherent mammalian cells. Exp Cell Res 317, 2384–2389.

Zonies S, Motegi F, Hao Y, Seydoux G (2010). Symmetry breaking and polarization of the C. elegans zygote by the polarity protein PAR-2. Development 137, 1669–1677.

Zou Y, Shao Z, Peng J, Li F, Gong D, Wang C, Zuo X, Zhang Z, Wu J, Shi Y, Gong Q (2014). Crystal structure of triple-BRCT-domain of ECT2 and insights into the binding characteristics to CYK-4. FEBS Lett 588, 2911–2920.

Supplemental Materials

Molecular Biology of the Cell

Zhuravlev et al.

Supplemental Information: Zhuravlev *et al.* 2017

Title

CYK-4 regulates Rac, but not Rho, during cytokinesis

Authors

Yelena Zhuravlev[1], Sophia M. Hirsch[1], Shawn N. Jordan[2], Julien Dumont[3], Mimi Shirasu-Hiza[1], and Julie C. Canman[2]*

Affiliations

[1]Columbia University Medical Center, Department of Genetics and Development, New York, NY 10032

[2]Columbia University Medical Center, Department of Pathology and Cell Biology, New York, NY 10032

[3]Institut Jacques Monod, CNRS, UMR 7592, Université Paris Diderot, Sorbonne Paris Cité F-75205 Paris, France

*Corresponding author: Julie C. Canman, 630 W. 168th St., New York, NY 10032, (212) 305-5017, jcc2210@cumc.columbia.edu

Running Head

CYK-4 and Rac in cytokinesis

Supplemental Information Table of Contents:

Supplementary Figure Legends

Figure S1: *cyk-4(ts) mutant embryos take longer to form a double membrane and fail in cytokinesis at the 2-cell stage via a Rac-dependent mechanism*

A) Time-lapse montage of the division plane region over time during cytokinesis in control and *cyk-4(ts)* mutant 1-cell embryos with and without *Rac(RNAi).* The plasma membrane is labeled with GFP::PH. B) Analysis of the time from anaphase onset to double membrane formation in embryos from the genotypes shown. All of the controls but only a few *cyk-4(ts)* mutant embryos have formed a double membrane at 150 sec post-AO due to the slower rate of contractile ring constriction in *cyk-4(ts)* mutants (*e.g.* Figure 1A and C). Error bars represent the SD; p-values were obtained by an unpaired, two-tailed t-test (Table S3). C) Schematic of the 2-cell *C. elegans* embryo indicating the anterior AB and posterior P1 cells; and bar graph showing cytokinesis completion/failure rates of AB and P1 cells in *cyk-4(ts)* mutant 2-cell embryos with or without *Rac(G60R)* at restrictive temperature. The number of embryos per genotype is indicated on each individual bar; p-values were obtained by both Fisher's and Barnard's exact tests (Table S3). AO=anaphase onset. n.s.=p>0.05; *=p<0.05; **=p<0.01; ***=p<0.001; ****=p<0.0001. Scale bars: yellow=60 sec, white=10 μm.

A

B

Semi-restrictive temp. (24°C)

Time from AO to
Double Membrane Formation

C

2-cell *C. elegans*
embryo

AB   P1

Restrictive temp. (25.5°C)

AB cell   P1 cell

cyk-4(ts) — 19 / 20

cyk-4(ts);Rac(G60R) — 14 / 16

% of embryos
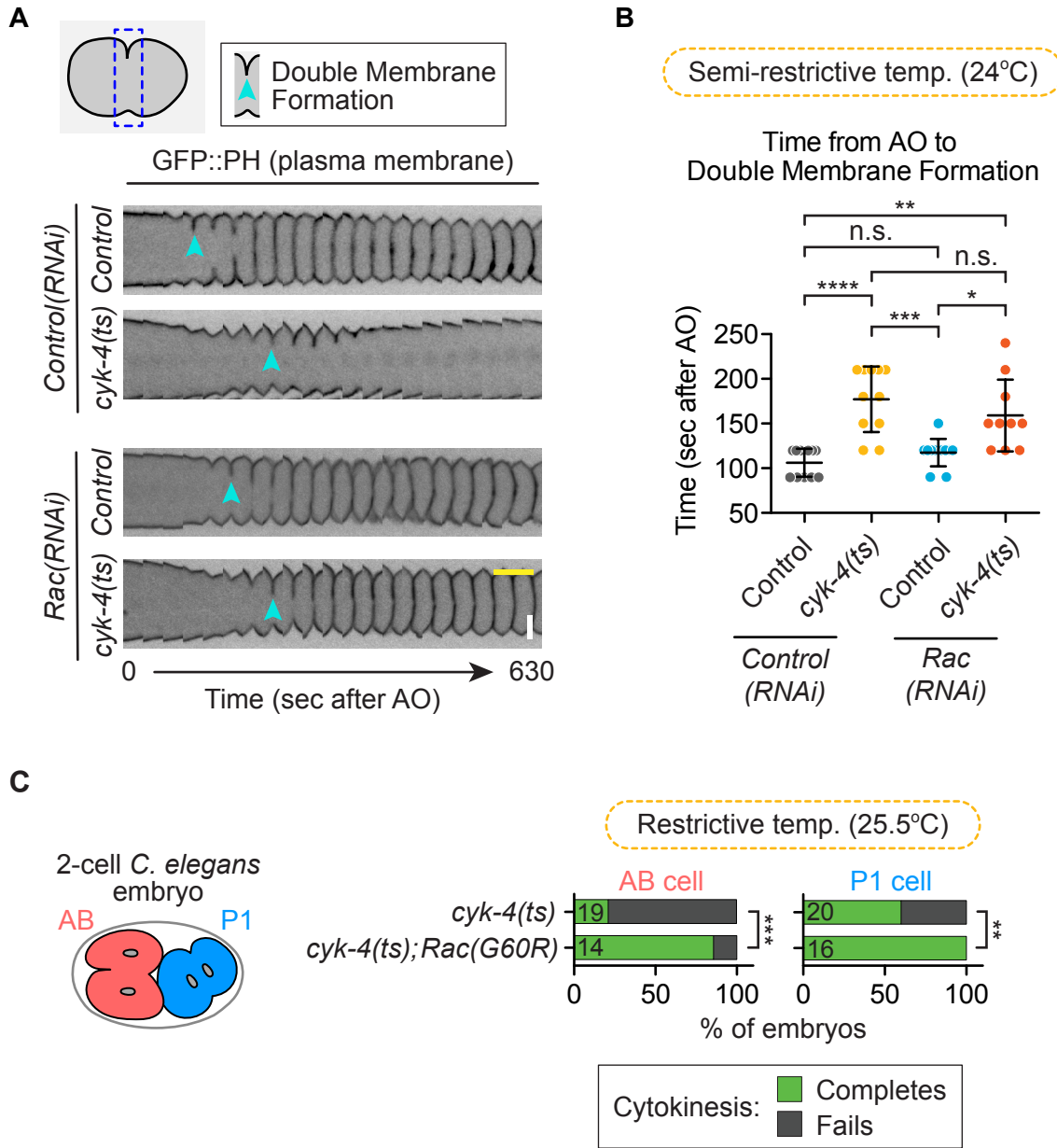
Cytokinesis: Completes / Fails

Figure S2: *Genetic model for Rho family GTPase signaling during cytokinesis*

Revised genetic model for the molecular regulation of Rho family small GTPases during cytokinesis. Note: We cannot rule out a role for ECT-2 in regulating Rac and/or CYK-4 activity. We also cannot rule out a role for ECT-2 and/or CYK-4 in regulating Cdc42 activity.
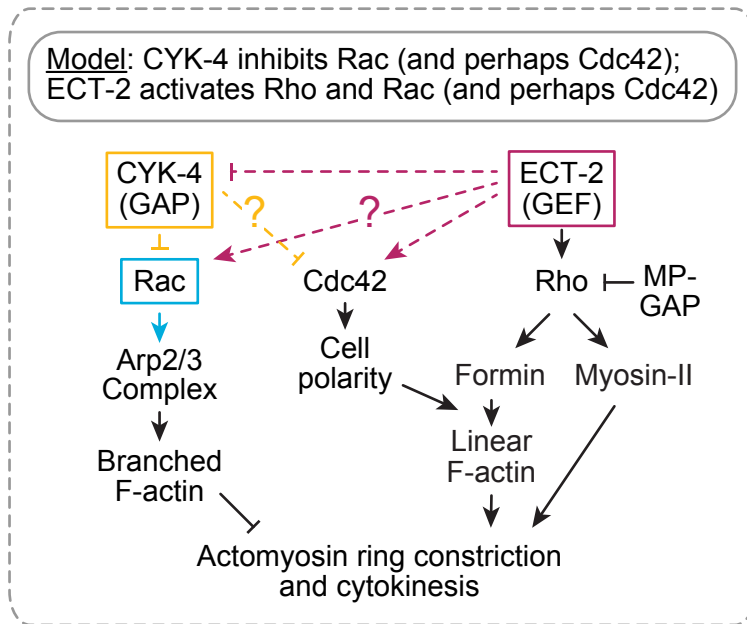
Supplementary Table Legends

Table S1: *Strain names and genotypes*

List of all strain names and genotypes used in this study.

Table S2: *Feeding RNAi constructs*

Plasmid names, oligos for RNAi feeding constructs, and DNA templates with the Ahringer clone number and/or cloning vector information used in this study.

Table S3: *Statistical analysis.*

Matrix of all statistical analysis, p-values, and experimental numbers used throughout this study.

Strain Names and Genotypes

Strain	Genotype
N2	*wild-type (ancestral)*
OD95	*unc-119(ed3)* ltIs38[pAA1; pie-1::eGFP::PH(PLC1delta1) unc-119(+)]III; ltIs37[pAA64; pie-1:: mCherry::his-58 unc-119(+)]IV*
JCC176	*unc-119(ed3)* ltIs38[pAA1; pie-1::eGFP::PH(PLC1delta1) unc-119(+)]III; ced-10(n3246)IV*
OD239	*cyk-4(or749ts) unc-119(ed3)* ltIs38[pAA1; pie-1::eGFP::PH(PLC1delta1) unc-119(+)]III; ltIs37[pAA64; pie-1::mCherry::his-58 unc-119(+)]IV*
JCC146	*cyk-1(or596ts) unc-119(ed3)* ltIs38[pAA1; pie-1::eGFP::PH(PLC1delta1) unc-119(+)]III; ltIs37 [pAA64; pie-1::mCherry::his-58 unc-119(+)]IV*
JCC177	*cyk-1(or596ts) unc-119(ed3)* ltIs38[pAA1; pie-1::eGFP::PH(PLC1delta1) unc-119(+)]III; ced-10(n3246)IV*
JCC192	*nmy-2(ne3409ts) dpy-5**; unc-119(ed3)* ltIs38[pAA1; pie-1::eGFP::PH(PLC1delta1) unc-119(+)]III; ltIs37[pAA64; pie-1::mCherry::his-58 unc-119(+)]IV*
JCC203	*nmy-2(ne3409ts), dpy-5**I; unc-119(ed3)* ltIs38[pAA1; pie-1::eGFP::PH(PLC1delta1) unc-119(+)]III; ced-10(n3246)IV*
JCC925	*ect-2(ax751ts)II; unc-119(ed3)*, ltIs38 [pAA1; pie-1::eGFP::PH(PLC1delta1) unc-119(+)]III*
JH2754	*ect-2(ax751ts)II*
MG592	*ect-2(ax751ts)II; ced-10(n1993)IV*
MT5013	*ced-10(n1993)IV*
JCC719	*mgSi3[cb-unc-119(+) eGFP:utrophin]III; unc-119(ed3)*III; ltIs37[pAA64; pie-1::mCherry::his-58 unc-119(+)]IV*
JCC765	*mgSi3[cb-unc-119(+) eGFP:utrophin]III; unc-119(ed3)* cyk-4(or749ts)III; ltIs37 [pAA64; pie-1::mCherry::his-58 unc-119(+)]IV*
JCC541	*unc-119(ed3)*III; ltIs37 [pAA64; pie-1::mCherry::his-58; unc-119(+)]IV; zuIs45[nmy-2:: nmy-2::eGFP unc-119(+)]V*
OD235	*unc-119(ed3)* cyk-4(or749ts)III; zuIs45[nmy-2::nmy-2::eGFP unc-119(+)]V.*
JCC178	*unc-119(ed3)* cyk-4(or749ts) ltIs38[pAA1; pie-1::eGFP::PH(PLC1delta1) unc-119(+)]III; ced-10(n3246)IV*
BA17	*fem-1(hc17)IV*
OD227	*cyk-4(or749ts)III*
EU1303	*cyk-4(or570ts)III*

*The *unc-119(ed3)* mutation was present in the parental strains but has not been directly sequenced in these strains to determine if the *unc-119* gene is mutated.

**The exact *dpy-5* allele is unknown but presumed to be *e61*, as published in (Carvalho *et al.* 2009. <u>Cell</u>. 137:936-37).

Table S2: Zhuravlev et al (2017)

Feeding RNAi constructs

Plasmid	Gene(s)	Oligo 1 (5'-3')	Oligo 2 (5'-3')	Template	Cloning vector
pJC90	*ced-10 (C09G12.8)*	GCGCG**AAGCTT** TCAAATGTGTCGTCGTTGGT	GCGCG**AAGCTT** GATCGCCTCATCGAAAACTTG	N2 cDNA	L4440 (empty vector)
pJC53	*cdc-42 (R07G3.1)*	Acquired from Ahringer library (Clone # II-5P13)			